

# Diagenetic controls on the reservoir quality of tight reservoirs in digitate shallow-water lacustrine delta deposits: An example from the Triassic Yanchang Formation, southwestern Ordos Basin, China

Zheng Yang<sup>a,b</sup>, Shenghe Wu<sup>a,b,\*</sup>, Jiajia Zhang<sup>a,b</sup>, Ke Zhang<sup>a,b</sup>, Zhenhua Xu<sup>c</sup>

<sup>a</sup> College of Geosciences, China University of Petroleum-Beijing, Changping, Beijing, 102249, China

<sup>b</sup> State Key Laboratory of Petroleum Resource and Prospecting, China University of Petroleum-Beijing, Beijing, 102249, China

<sup>c</sup> College of Geosciences, Yangtze University, Wuhan, Hubei, 430100, China

## ARTICLE INFO

### Keywords:

Tight sandstone reservoir  
Diagenesis  
Reservoir quality  
Digitate shallow-water lacustrine delta  
Bar finger  
Architectural bounding surface

## ABSTRACT

Diagenesis is a very important factor to determine the quality of clastic reservoirs, especially in tight sandstone reservoirs. The tight reservoir of Triassic Yanchang Formation in southwestern Ordos Basin is the foremost hydrocarbon exploration target. The shallow-water lacustrine delta developed in Chang 8 reservoir of the study area is distributed in digitate shape, which are mainly composed of distributary channel, continuous mouth bar and together with natural levee above. The typical tight reservoir of Chang 8 member experienced a complex diagenetic evolution process, but the relationship among diagenetic alteration, deposits and lithofacies, as well as their control and influence on reservoir quality is still unclear. In this study, casting thin section, scanning electron microscope (SEM) and backscatter scanning electron microscope (BSE) combined with energy spectrum analysis, together with stable isotope analysis, X-ray diffraction analysis, and homogenization temperature test of fluid inclusions are used to analyze the reservoir characteristics including petrology, lithofacies, history and intensity of diagenesis. The control and influence of these characteristics on ultimate reservoir quality of digitate shallow-water lacustrine deltas are further evaluated. The results show that four lithofacies can be identified (namely, “i”, “ii”, “iii”, “iv”) with the decrease of grain size and increase of ductile components in the tight sandstones of digitate shallow-water lacustrine delta, respectively corresponding to preferential development positions in the deposits. There are similarities and differences on the diagenetic processes among various lithofacies. The strong mechanical compaction after burial primarily decrease the original pore space in all lithofacies, and the largest loss of pore space occurs in lithofacies iv sandstones (siltstone with wavy bedding). The chlorite is mainly in the morphology of pore-lining, but coating and rosette-like chlorite are rare. The ability to resist compaction in sandstones of lithofacies i and lithofacies ii is enhanced due to the moderate development of pore-lining chlorite, thus retaining partial pore space. Carbonate cements are abundant in relatively coarser-grained sandstones close to the sandstone-mudstone interface, and the occurrence of these cements is closely related to the adjacent mudstone, indicating that Fe and Mg ions necessary for carbonate cementation are most likely from adjacent mudstone where ions are released by mechanical compaction and subsequent hydrocarbon generation pressurization during the burial process. Weak carbonate cementation occasionally occurs at the architectural bounding surface far away from mudstone, which probably related to the transformation of clay minerals. Five typical diagenetic evolution patterns in digitate shallow-water lacustrine deltaic reservoir are summarized by considering the diagenetic processes with deposits and lithofacies. From pattern I to pattern V, the corresponding reservoir quality gradually deteriorates. The results in this study are of great help to deepen the understanding of diagenetic alteration process and reservoir heterogeneity of tight sandstones, and provide theoretical basis for exploration and sustainable development of similar lacustrine shallow-water lacustrine delta reservoirs, especially for bar fingers in shallow-water deltas.

\* Corresponding author. College of Geosciences, China University of Petroleum-Beijing, Changping, Beijing, 102249, China.

E-mail addresses: [2019310028@student.cup.edu.cn](mailto:2019310028@student.cup.edu.cn) (Z. Yang), [reser@cup.edu.cn](mailto:reser@cup.edu.cn) (S. Wu).

<https://doi.org/10.1016/j.marpetgeo.2022.105839>

Received 20 February 2022; Received in revised form 13 July 2022; Accepted 14 July 2022

Available online 4 August 2022

0264-8172/© 2022 Elsevier Ltd. All rights reserved.

## 1. Introduction

With the decline of conventional hydrocarbon productivity, unconventional reservoirs especially tight reservoirs, characterized by horizontal well drilling and hydraulic fracturing, are becoming increasingly important substitutes for global oil and gas sustainable supply. Tight oil reservoirs refer to unconventional oil-bearing rocks with extremely low porosity and permeability (lower than 10% and 1mD, separately) in China (Wang et al., 2018).

Tight reservoir of shallow-water lacustrine delta is one of the key fields of academic research and reservoir development over the years. According to various classification basis, the shallow-water lacustrine delta has been divided into different types (Fisk, 1954; Jopling, 1966; Donaldson, 1974; Postma, 1990; Olariu and Bhattacharya, 2006; Edmonds and Slingerland, 2010; Edmonds et al., 2011), for instance, digitate (or bird-foot shaped) and lobate shallow-water lacustrine delta based on the morphology of sand bodies, distributary channel dominated and distributary bar dominated separately based on the morphology of sand body framework (Bernard, 1965; Fisher et al., 1969; Dumars, 2002; Burpee et al., 2015; Xu et al., 2019, 2022). The distribution and characteristics of deposits and lithofacies in different types of shallow-water lacustrine deltas are different. Digitate (bird-foot shaped) shallow-water lacustrine delta tight reservoirs are found in many basins and modern sedimentation in China, including Ordos Basin (Hu et al., 2008; Chen et al., 2016), Songliao Basin (Zhu et al., 2017), Bohai Bay Basin (Zhang et al., 2017; Hu et al., 2019; Xu et al., 2019), Ganjiang delta in Poyang Lake (Wu et al., 2019; Xu et al., 2022), Dongting Lake (Yin et al., 2012), etc.

Different from the conventional bird-foot shallow-water lacustrine delta simply dominated by distributary channels, Chang 8 reservoir in Maling oilfield of Ordos Basin includes not only distributary channels on the delta plain, but also continuous forward elongate compound sand body in delta front. The compound sand body consists of three different deposits: continuously distributed mouth bar, upper undercutting distributary channel and natural levee deposits distributed on both sides of the channel. This kind of combination of deposits is called “bar finger”, which is the unique feature of shallow-water lacustrine delta in this study. Due to the development of the digitate compound sand body in the front of shallow-water lacustrine delta, the types of lithofacies are also different from that of the shallow-water lacustrine delta simply dominated by distributary channels (Li et al., 2017; Deng et al., 2019). Previous scholars have done much research on the reservoir quality of shallow water delta only composed of distributary channel and front mouth bar at the end of the channel, which mainly focused on heterogeneity and classification of pore structure (Qiao Juncheng et al., 2020; Li et al., 2017), diagenetic sequence of diagenetic minerals, influence of various diagenetic minerals on reservoir quality, etc. Burial history, tectonic movement, mineral constituent and early mineral cementation of the original sediments are supposed to be key effect factors of compaction (Loucks et al., 1984; Chuhan et al., 2000, 2003; Trendell et al., 2012; Fu et al., 2013; Bjørlykke, 2014). Although predecessors have studied the diagenesis characteristics of the reservoir in bar fingers and divided the diagenetic facies of Maling area (Zhang et al., 2004; Wang et al., 2020), the relationship among diagenesis, deposits, lithofacies and final reservoir quality has not been systematically studied or reported. In addition, there are few reports on the distribution and evolution patterns of diagenesis related to deposits and lithofacies of tight sandstone reservoirs in digitate shallow-water lacustrine delta.

Taking the Upper Triassic Chang 8 tight reservoir in Maling oilfield of southwestern Ordos Basin as the research object, this study is designed in order to investigate the divergence of diagenetic alteration linked to various depositional facies as well as lithofacies in digitate shallow-water lacustrine delta reservoir, and to explicit the controlling factors of different diagenetic processes on reservoir quality. For the sake of characterizing the micro characteristics of diagenetic alteration of the reservoir, including the duration and sequence of diagenetic

minerals, material source of diagenetic minerals, strength of different diagenesis, various techniques and methods are integrated in this study such as core observation and description, casting thin section fabrication and examination, observation of scanning electron microscope (SEM) and backscatter scanning electron microscope (BSE), XRD analysis of clay minerals, homogenization temperature test of fluid inclusions and stable carbon isotope analysis. More importantly, the final research results are expected to provide reference and ideas for international academic research and hydrocarbon development of similar delta reservoirs.

## 2. Geological settings

Ordos Basin, located in north-central China, occupies an area of more than  $25 \times 10^4 \text{ km}^2$  (Fig. 1). The basin is bounded by four large mountains and its interior has been subdivided into six tectonic units considering the structural characteristics, namely Yishaan Slope, the Jinxi Flexure Zones, Yimeng Uplift, Weibei Uplift, the Tianhuan Syncline and the Western Thrusted zone. The basin strata cover the deposits from Late Proterozoic to Mesozoic (Middle Jurassic, specifically). Before Mesozoic, the basin was dominated by marine sediments. Ordos basin entered the development stage of inland lake basin during Mesozoic, among which the Late Triassic (Yanchang period) was the peak period (Zhu et al., 2013; Zou et al., 2010).

Considering marker beds, sedimentary cycles and lithological association, the Upper Triassic Yanchang Formation is subdivided into 10 oil-bearing intervals from Chang 10 interval at the bottom to Chang 1 interval at the top (Deng et al., 2008; Duan et al., 2008; Yao et al., 2009; Lai et al., 2016; Zhou et al., 2016) (Fig. 2). The Yanchang Formation covers a complete cycle of lake evolution in the vertical facies succession, which can be summarized into three main stages (Zou et al., 2010; Liu et al., 2013). Chang 10-Chang 7 is the formation period of the lake basin, and the lake development reaches its climax in Chang 7 period. Chang 6-Chang 3 is the development period of delta construction, and the lake basin began to shrink concurrently. The lake basin continued to shrink and ultimately disappeared during Chang 2-Chang 1. Here the studied sandstones came from Chang 8 interval, which are in conformity with the overlying Chang 7 interval and underlying Chang 9 interval.

As a reservoir adjacent to the source rock, the hydrocarbon in Chang 8 sandstones mainly came from the overlying source rock of Chang 7 member. Considering the fractures in the study area are not developed, the hydrocarbon generated after the maturity of Chang 7 source rock mainly migrated downward through the pore system of Chang 8<sub>1</sub> sandstones due to hydrocarbon-generating pressurization, forming a set of source-reservoir-seal rock assemblage of “upper-generation and lower-storage” (Chu et al., 2013).

The burial history shows that the Yanchang Formation experienced four uplifting processes after burial and reached the maximum burial depth about 90 Ma ago (Fu et al., 2013) (Fig. 3). The burial depth of Chang 8 varies from 1400 m to 2800 m, and the thickness is about 85–95 m. According to formation thickness and secondary sedimentary cycles, the Chang 8 interval is subdivided into Chang 8<sub>2</sub> and Chang 8<sub>1</sub> from bottom to top, of which Chang 8<sub>1</sub> is the main oil-bearing unit (Yao et al., 2013). The Chang 8<sub>1</sub> oil-bearing unit consists of Chang 8<sub>1</sub><sup>1</sup>, Chang 8<sub>1</sub><sup>2</sup> and Chang 8<sub>1</sub><sup>3</sup>, and this paper focuses on the third layer Chang 8<sub>1</sub><sup>3</sup> in which sand bodies are the most developed.

The study area – Maling Oilfield, covering an area of approximate  $7 \times 10^2 \text{ km}^2$ , is located in the middle of Maling area, which stretches across Tianhuan Syncline and Yishaan Slope in southwestern Ordos Basin (Fig. 1). Chang 8 member in the oilfield is an extremely gentle west dipping monocline with inclination less than  $0.7^\circ$ , and faults and folds are almost undeveloped. The study area is mainly controlled by the southwest provenance and sedimentary system during the formation and evolution of the studied interval.

Combined with the characteristics of stable sedimentary structure, large area, shallow water depth and gentle slope, as well as biological

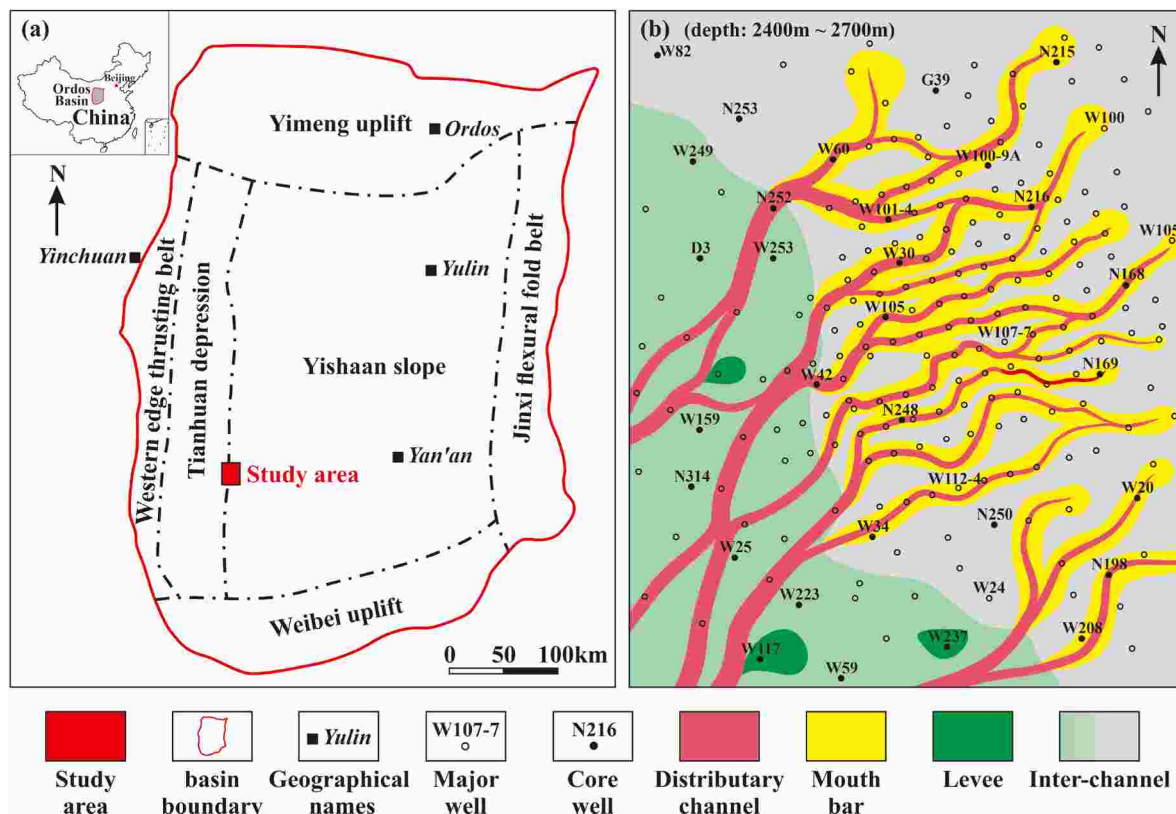


Fig. 1. (a) Geological background and location of Maling Oilfield. (b) Map showing the distribution of dominant deposits of submember Chang 8<sub>1</sub> in the study area.

and geochemical indicators, it is considered that the sedimentary environment of Chang 8 reservoir in Maling oilfield is a shallow-water delta system, which mainly consists of four major deposits – distributary channel, mouth bar, natural levee and interdistributary bay (Yang et al., 2015). However, it may not be a simple lobate shaped or traditional bird-foot delta in morphology. In this work, the spatial combination of distributary channel, mouth bar, natural levee in lower plain and front of the delta is more like a finger shape, which is called “bar finger” (Fisk, 1954; Donaldson, 1969).

When it comes to reservoir properties, due to the deep burial process and complex diagenesis, the Chang 8<sub>1</sub> member is now a tight reservoir with ultra-low permeability (Wang et al., 2017; Zhu et al., 2017). The porosity of the reservoir measured by core analysis ranges from 1.5% to 15.9%, with an average of 8.6%, of which most are no more than 12% (Fig. 4). The permeability varies from 0.001 mD to 15.35 mD, with a logarithmic average of 0.58 mD, and more than 86% of the samples display permeability less than 1mD (Fig. 4).

### 3. Samples and methods

In this study, 187 m cores from 30 wells of Chang 8 tight reservoir were observed and detailed described (location of the wells were marked in Fig. 1). 117 broken core samples from 10 wells were collected, 45 of which were also taken as core column samples concurrently. All core sections have been depth-normalized by comparing gamma curves.

117 samples were analyzed by X'pert MPD X-ray diffractometer with Cu-K $\alpha$  radiation and operated separately at 100 mA and 40 kV to determine the types, relative and absolute contents of clay minerals and the ratio of illite to montmorillonite (I/S).

A total of 82 core plug samples and some broken samples were used for manufacturing casting thin sections and SEM/BSE samples. For purpose of identifying the pores and carbonate minerals more clearly

under the microscope, blue epoxy resin and Alizarin Red S dye were injected during preparation of casting thin sections. The petrographic characteristics (mineral composition and content, grain size, sorting coefficient, roundness, matrix content), pore structure characteristics (pore morphology and percentage of total rock volume), morphology and contact relationship of diagenetic minerals in pores can be identified through observation and point count of 300 points in each sample under optical polarization microscope (Olympus BH2). In order to observe under microscope more clearly and reduce the influence of surface roughness, samples for SEM prefer to be that of fresh broken section with gold sprayed, and the BSE samples were polished by Arion milling through the use of the Leica EM TIC 3X Ion Beam Milling system.

16 samples from carbonate cemented sandstones and adjacent mudstones from 6 wells were selected for testing stable carbon and oxygen isotope, which can be used to determine the source of carbonate minerals. Carbon dioxide gas was released during the acidification process of samples, which can be used to gain the data of carbon and oxygen isotope, and the results are expressed in standard  $\delta$  notation according to the V-VPD (Vienna PeeDee Belemnite) standards.

8 thicker sections were made to analyze the petrological characteristics and measure the homogenization temperature of mineral fluid inclusions. The homogenization temperature was measured under Leica microscope on LINKAM THSMG 600 cooling-heating stage. The experimental conditions included that a heating rate of 10 °C per minute at temperature lower and higher than 60 °C respectively, and the accuracy of the measured results was  $\pm 1$  °C.

### 4. Results and interpretation

#### 4.1. Petrography

On the basis of drill cores observation and statistical analysis of casting thin sections, the rock types of Chang 8 reservoir are mainly

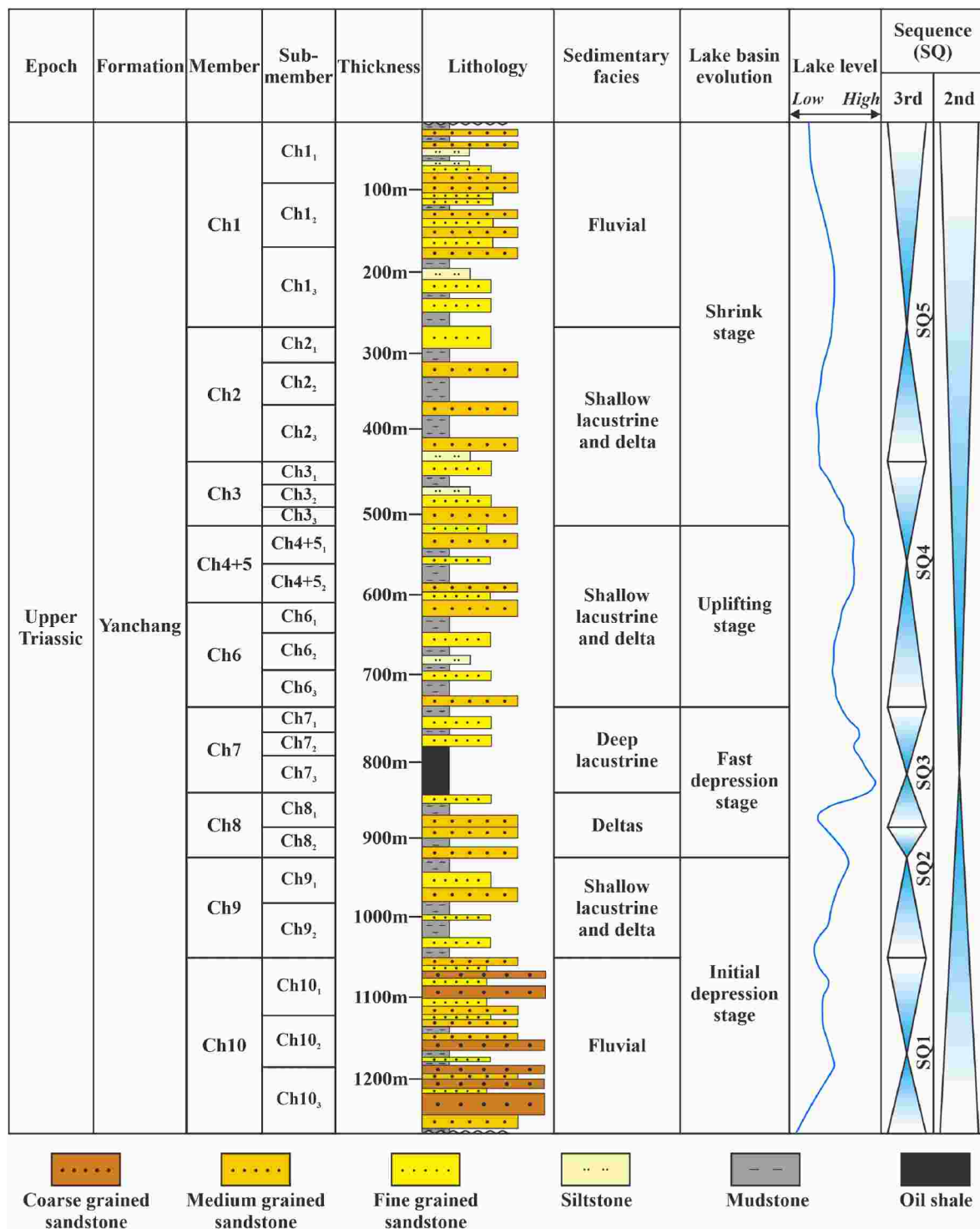


Fig. 2. Simplified stratigraphic column showing the lithology, thickness and sequence of Upper Triassic Yanchang Formation (modified from Zhou et al., 2016).

lithic arkose (63.5%), followed by feldspathic litharenite (27.6%). The average framework proportion is  $Q_{36.8}F_{35.3}R_{27.9}$  according to Folk's classification scheme (Folk, 1968), and the compositional maturity is generally low (Fig. 5). Quartz is the major detrital component, with a relative content ranging from 18% to 57%. The content of feldspar is in the range of 12% and 61%, mainly comprised of plagioclase and K-feldspar. Additionally, the detrital components contain lithic fragments, ranging from 9% to 46%, which are composed of metamorphic rock fragments (avg. 14%), volcanic rock fragments (avg. 9%) and rare sedimentary rock fragments (less than 3%). Furthermore, mica accounts

for 5.2% of the total rock volume in Chang 8<sub>1</sub> tight sandstones, including muscovite and a small amount of biotite.

Grain size of detrital particles varies from medium-grained (0.02–0.5 mm) to silt-grained (0.01–0.1 mm) sand. These sandstones are mostly characterized by moderate-good sorting and subangular grain shape, hence their textural maturity is medium. The grain-contacts are mainly linear contacts and some concave-convex contacts due to high content of plastic minerals such as mica and some soft rock fragments.



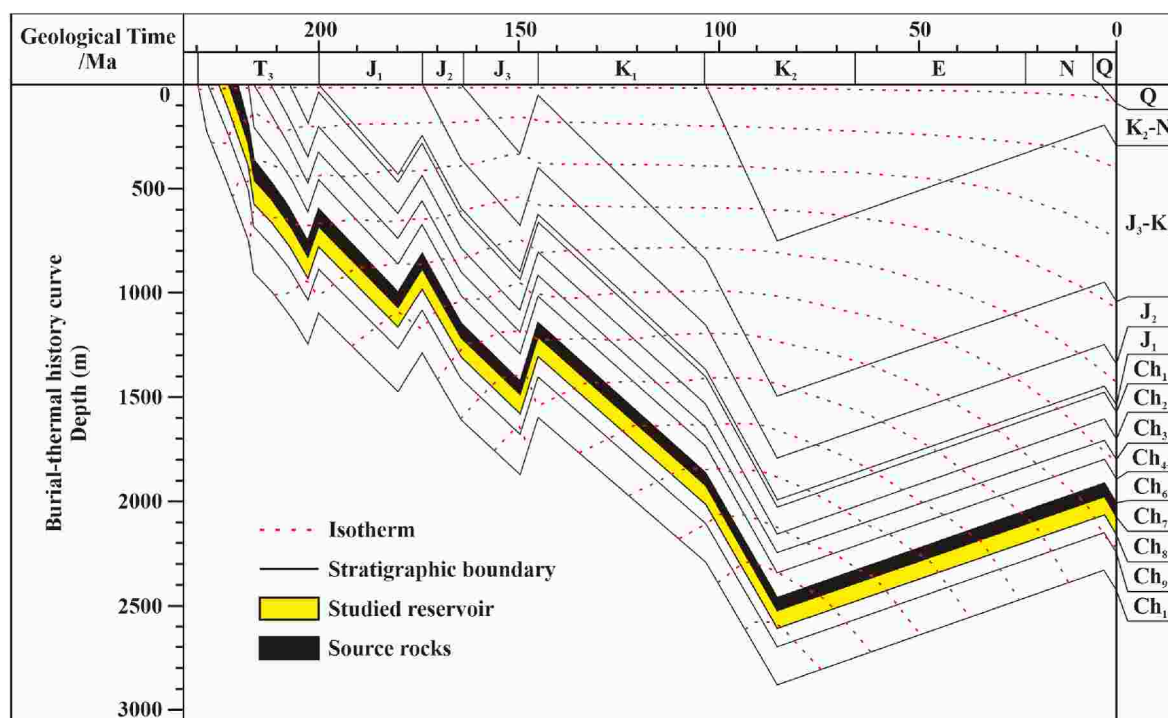


Fig. 3. Burial-thermal history of the Triassic Yanchang Formation (after Fu et al., 2013).

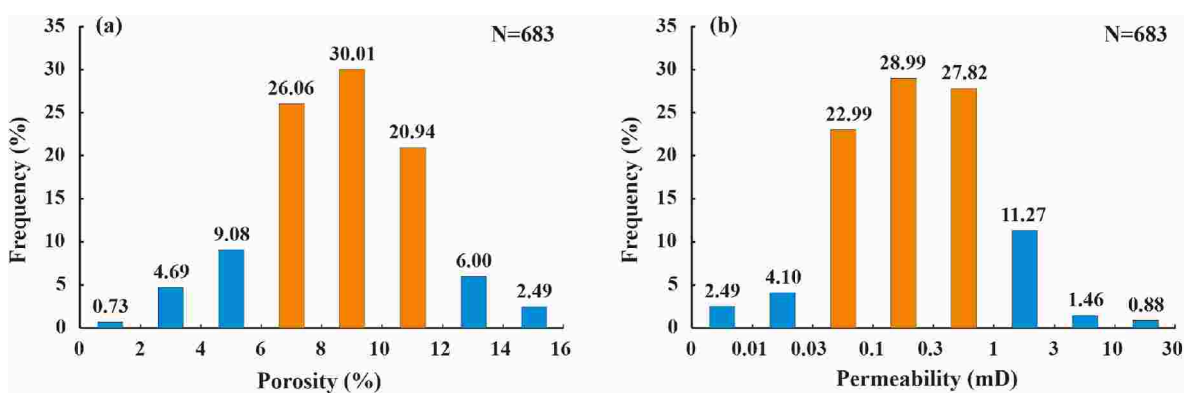


Fig. 4. Histogram illustrating the distribution intervals of reservoir petrophysics: (a) porosity, (b) permeability.

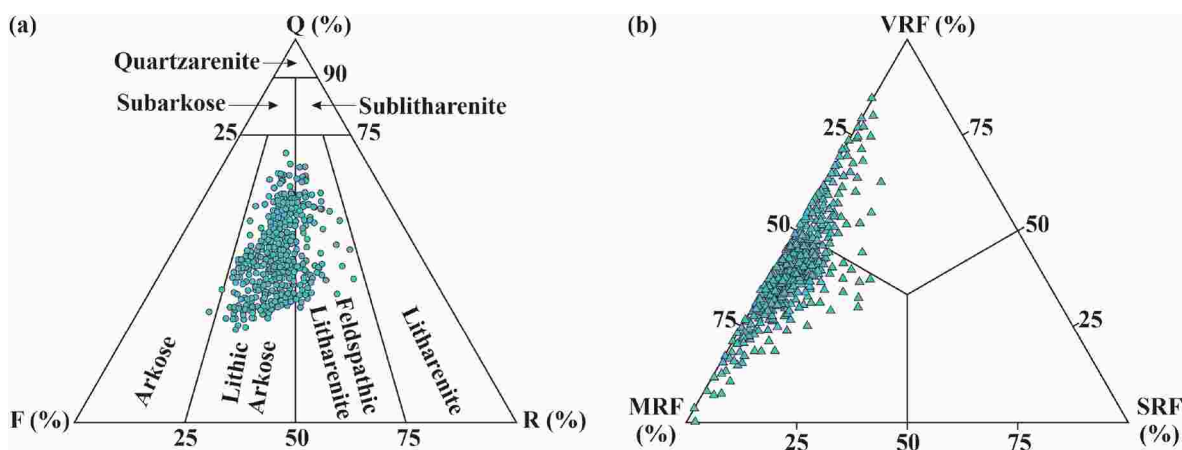


Fig. 5. Petrographic characteristics of the studied sandstones in Chang 8<sub>1</sub> reservoir: (a) QFR detrital composition plotted on Folk's (1968) ternary diagram. Q = quartz, F = feldspar, R = rock fragments; (b) Ternary diagram demonstrating the compositions of rock fragments. VRF = volcanic rock fragments, MRF = metamorphic rock fragments, SRF = sedimentary rock fragments.

4.2. Lithofacies

Generally, the reservoir quality varies with lithofacies, and the distribution of lithofacies is controlled by deposits. In accordance with the characteristics of grain size and content of ductile components observed by thin sections, together with sedimentary structures observed from cores, four main lithofacies were identified in bar fingers of shallow-water lacustrine delta in Chang 8<sub>1</sub> tight sandstone reservoir (Table 1).

- (i) Medium-fine grained, cross-bedded sandstones with extremely low content of ductile components

Sandstones of this lithofacies are medium-fine grained and characterized by parallel bedding, cross bedding of wedge-shape or trough-shape. Samples of this kind of sandstone are relatively well sorted with low content of ductile components (such as soft rock fragments, biotite, muscovite, etc) and matrix (avg. 10% and 18%, respectively). This lithofacies is ubiquitous in the main part of distributary channels (except for the top) in upper delta plain, as well as the bottom of distributary channel of the bar finger in the lower plain and front of the delta, with a thickness ranging from 2 m to 8 m (②, ⑥ in Fig. 6a; and ② in Fig. 6b). In addition, carbonate cementation usually occurred in lithofacies i sandstones near the sandstone-mudstone interface (⑥ in Fig. 6a).

- (ii) Fine-grained, massive to parallel bedded sandstones with relatively low content of ductile components

Sandstones of this kind of lithofacies are considered to be fine-grained and relatively moderately-well sorted with massive bedding developed, and ductile components are rare with a content of averaging 16%. Lithofacies ii were sampled more frequently in cores and casting thin sections than lithofacies i, and usually appears at the top of distributary channels in the upper plain, mouth bar and the main part of channel (except for the bottom) of bar fingers in the lower plain and front of the delta, with a thickness interval of 1 m–6 m (③ in Fig. 6a; ① in Fig. 6b; ②, ④, ⑤ and ⑦ in Fig. 6c).

- (iii) Coarse siltstones to fine-grained sandstones with medium content of ductile component

Relatively finer grain (coarse silt to fine-grained) and inconspicuous bedding developed are the typical characteristics of sandstones of lithofacies iii owing to the weak hydrodynamic conditions, and they are relatively moderately sorted with medium content of ductile components (avg. 25%) compared with the above two lithofacies. The edge of distributary channel is the main place for the occurrence of such lithofacies (⑦ in Fig. 6a; and ④ in Fig. 6b).

- (iv) Siltstones with ripple lamination and high content of ductile components

Unlike the other three lithofacies, lithofacies iv possessed the finest grain size which is siltstones and high content of matrix and ductile components (>35% and >30%, respectively). This lithofacies mainly occurs in the natural levee deposits, where ripple lamination are occasionally seen (③ in Fig. 6a; ③ in Fig. 6b; and ①, ③ in Fig. 6c).

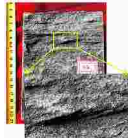
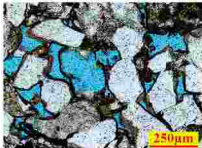

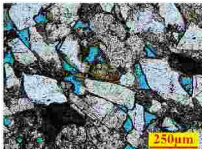



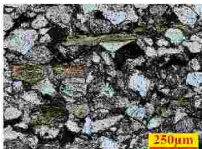
4.3. Types and characteristics of diagenesis

The occurrence of diagenesis not only changed the arrangement of detrital particles and the attachment of cements, but also affected the changes of primary pores and secondary pores that greatly determined the ultimate petrophysics of reservoirs. The analysis data of casting thin sections, SEM and XRD show that the Chang 8 reservoir has experienced serious diagenetic alteration since buried, marked by mechanical compaction, complex cementation and dissolution of eutectic minerals. The influence of various diagenesis on reservoir petrophysics differs a lot.

4.3.1. Mechanical compaction

The observation of casting thin sections shows that Chang 8 reservoir has undergone relatively strong compaction, which is mainly manifested by the strong bending and deformation of ductile minerals such as argillaceous debris and mica in sandstones (Fig. 7a), as well as the

**Table 1**  
Lithofacies classification of Chang 8<sub>1</sub> tight sandstones in Maling area.

Lithofacies	Petrography and sedimentary structures	Developmental position	Core photographs	Photomicrographs of casting thin sections
i	Mid-fine grained, cross-bedded, extremely low content of ductile components	Main part of distributary channel		
ii	Fine grained, massive-bedded, relatively low content of ductile components	Top of distributary channel and mouth bar of bar fingers		
iii	Coarse silt to fine grained, medium content of ductile component	Edge of distributary channel		
iv	Siltstones, ripple lamination, high content of ductile components	Natural levee		

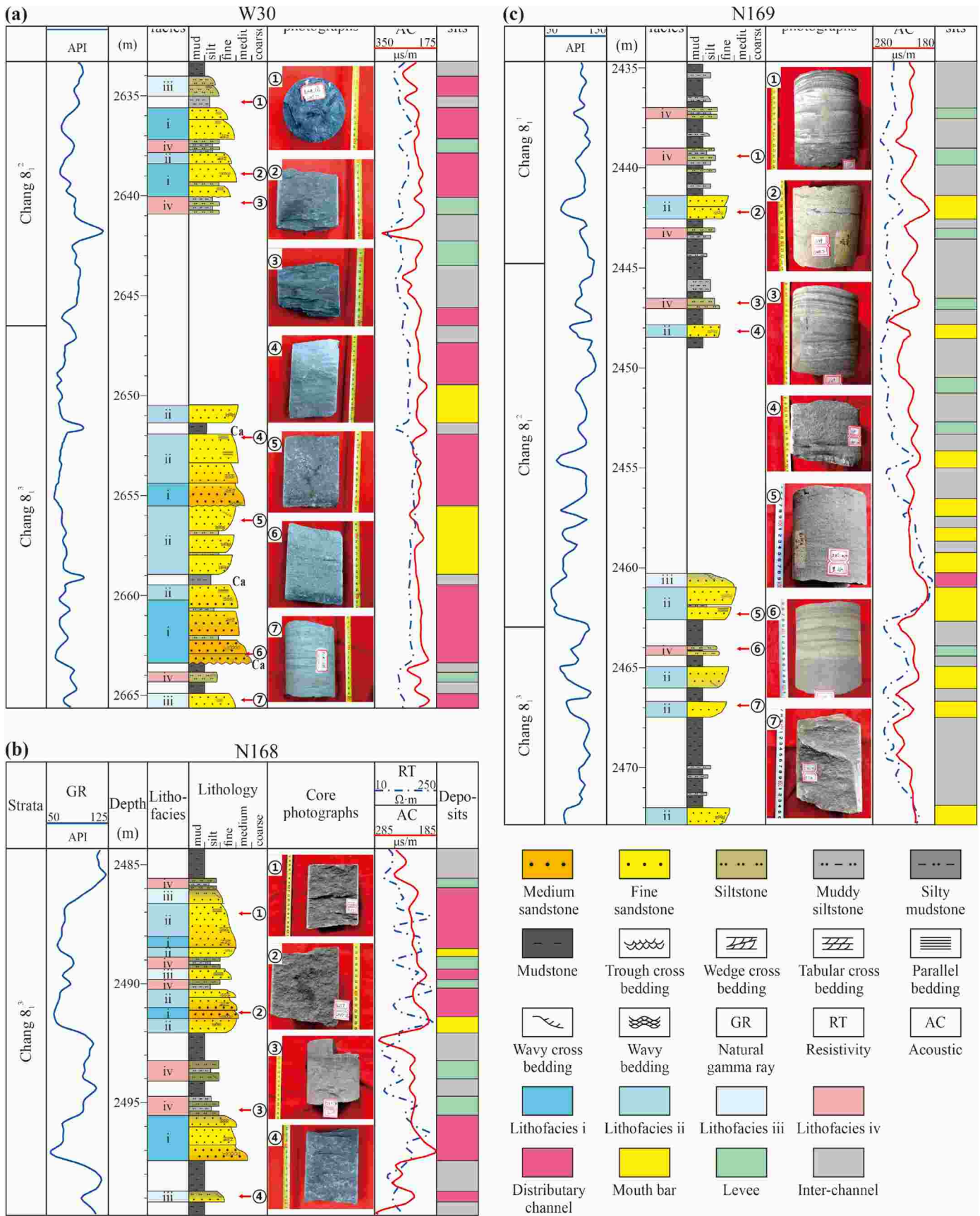
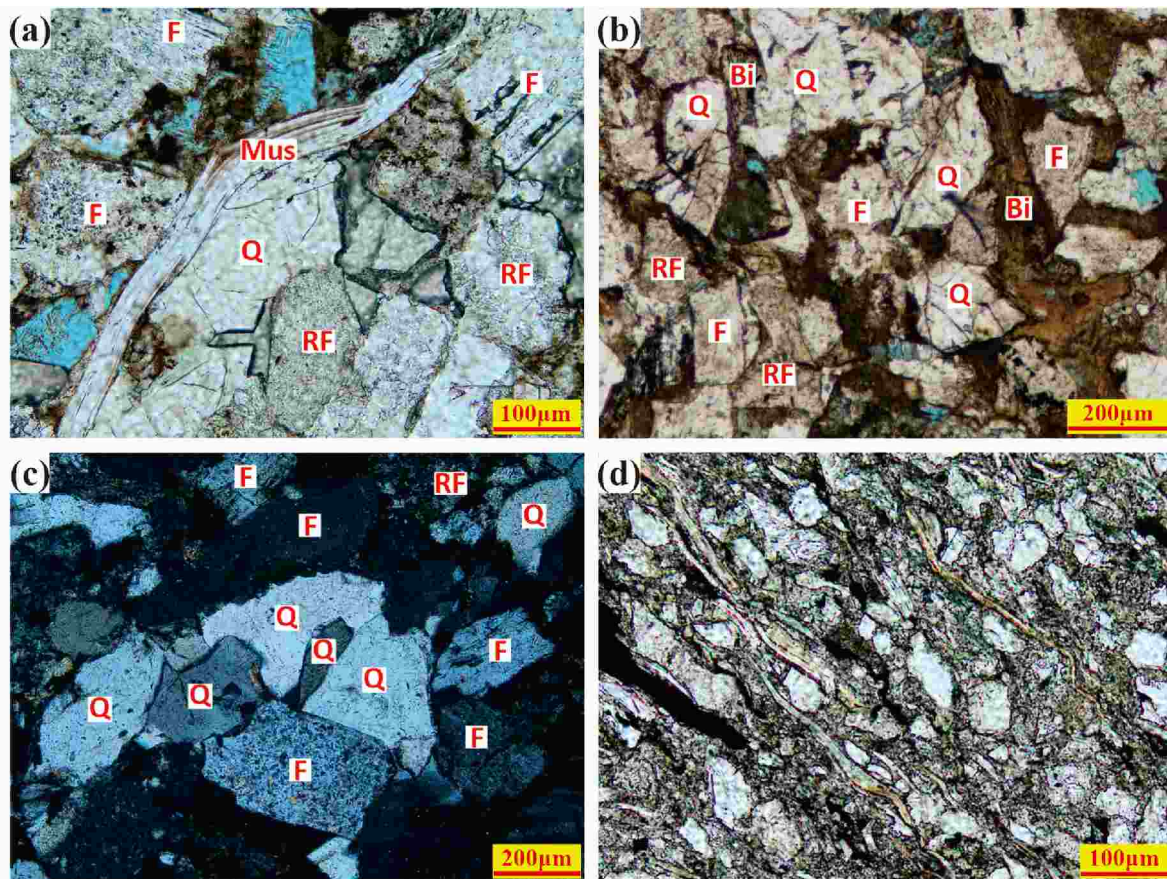


Fig. 6. Lithostratigraphic plots for cores from (a) well W30, (b) well N169, and (c) well N168. The locations are shown in Fig. 1b.





**Fig. 7.** The micrographs of casting thin sections showing different mechanical compaction characteristics in Chang 8 tight reservoir. (a) bending deformation of muscovite sheet (PPL, well W30d, 2641.4 m). (b) Crushing of rigid particles due to compaction (PPL, well W30, 2639.2 m). (c) compaction fracture and linear to concave-convex contact between quartz grains (XPL, well N168, 2484.24 m). (d) directional arrangement of minerals (PPL, well W30, 2638.38 m).

fracture of rigid minerals such as detrital quartz and feldspars (Fig. 7b). The detrital grains show a tendency of directional array locally after strong compaction, and the contacts between them is mainly linear or concave-convex (Fig. 7c and d). Compaction resulted in dense grain arrangement and reduction of primary intergranular pores, which greatly reduced original pore space of the reservoir.

#### 4.3.2. Cementation

According to the observation of thin sections, SEM and BSE micrographs, the composition of cements in Chang 8 reservoir is complex. The main cements mainly consist of carbonate cements (avg. 53%), authigenic clay minerals cements (avg. 37%) and siliceous cements (avg. 10%). On the one hand, cementation generally damages original and secondary pore, thus increasing the intensity of heterogeneity. In some cases, cements may improve the compressive resistance of detrital grains and provide the material basis of later dissolution.

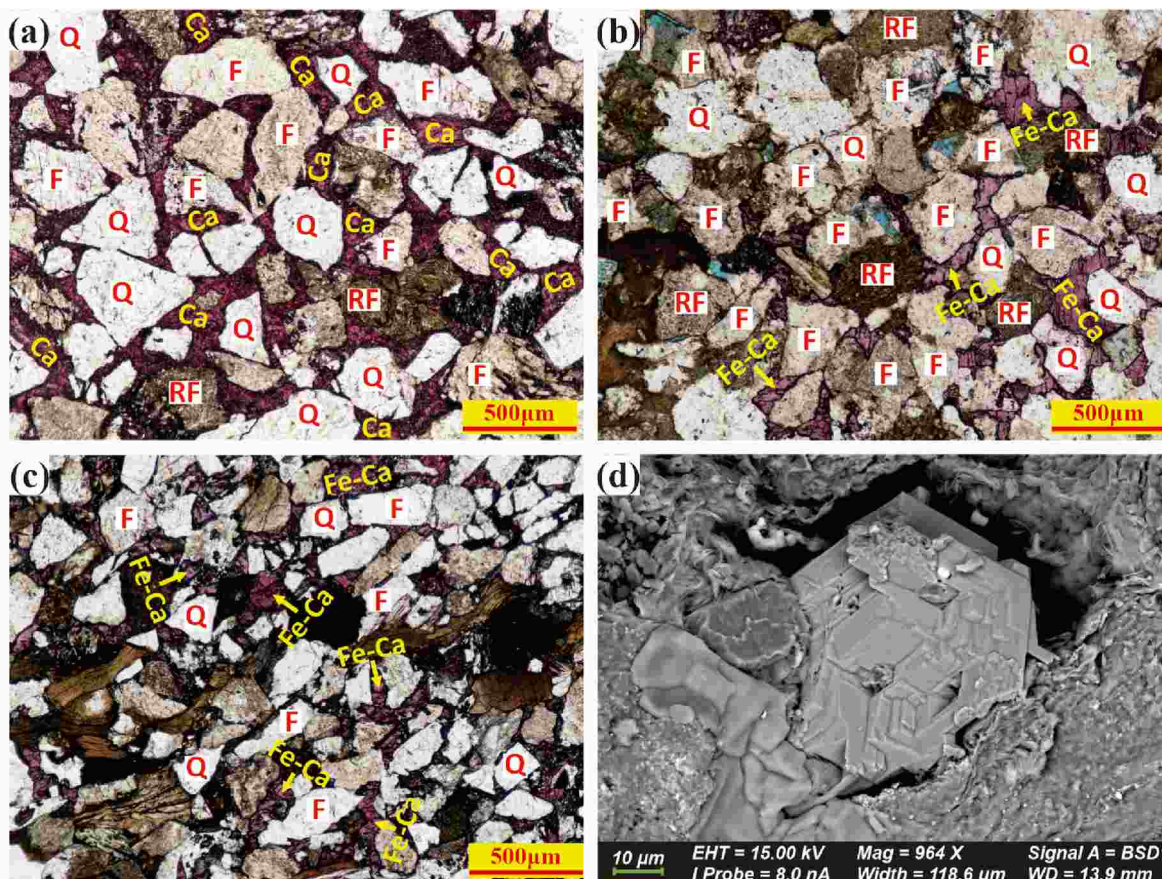
**4.3.2.1. Carbonate cementation.** In the Chang 8<sub>1</sub> strata of Maling Oil-field, carbonate cements are the most destructive cement type, which are widely distributed. The volume fraction of carbonate cements varies from 1% to 61.8%, with an average of 8.96%, which is much higher than other cements. Carbonate cements mainly consist of calcite and ferrocalcite, followed by dolomite and ferrodolomite, and occasionally with siderite. Calcite cements normally formed in the early diagenetic stage, filling the intergranular pores as argillaceous or microcrystalline forms, and were dyed bright red in casting thin sections (Fig. 8a). Ferroc carbonate cements, including ferrocalcite and ferrodolomite, generally formed later than carbonate cements. Ferrocalcite often cemented the pores in the form of continuous crystals, which was purplish red in

casting thin sections (Fig. 8b and c) whereas most of the ferrodolomite occurred with mosaic crystals' form and was colorless (Fig. 8d). Ferrocalcite and ferrodolomite not only cemented intergranular pores and early formed calcite, but also replaced feldspar and rock fragments (Fig. 8c), thus forming isolated irregular debris particles. Carbonate cements, which dominated by calcite and ferrocalcite, often filled intergranular and intragranular pores, leading to the decrease of effective pores and throats, which is one of the important factors causing Chang 8 sandstone tight.

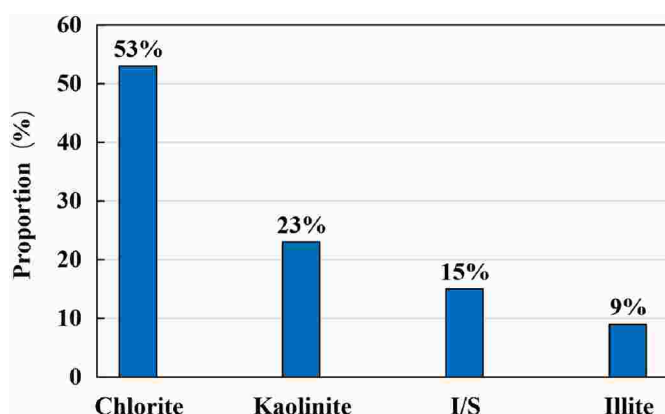
**4.3.2.2. Authigenic clay minerals cementation.** Except for carbonate cementation, clay mineral cementation is another type of most widely distributed cementation, occupying 3%–15% of the total rock volume and averaging 14%. Four main types of authigenic clay minerals were revealed by SEM observation and XRD analysis: chlorite, kaolinite, illite-smectite mixed-layer (I/S) and illite (Fig. 9). Among them chlorite is the most widespread composition (35%–68% and averaging 53% of the total clay volume), followed by kaolinite and I/S mixed-layer (relatively 8%–46% averaging 23%, and 3%–22% averaging 15% of the total clay volume, respectively). Illite is the rarest, accounting for 0.5%–15% (with a mean of 9%) of the clay minerals and it's almost absent in SEM and BSE images.

Authigenic chlorite observed by SEM and BSE mainly occurred in three different morphologies: (i) fine-sized coated chlorite growing parallel to the surface of detrital grains such as detrital quartz, with a thickness generally less than 2 µm (Fig. 10a), (ii) continuous or discontinuous coarse-sized pore-lining chlorite growing perpendicular to the surface of detrital grains, ranging in thickness from 2 to 10 µm, and invisible at the contacts between detrital grains (Fig. 10a and b), (iii)





**Fig. 8.** The micrographs of casting thin sections showing carbonate cementation characteristics in Chang 8 tight reservoir. (a) Equine denticulate bright-red calcite cements filling intergranular pores (PPL, well N216, 2550.35 m). (b) purplish red ferrocalcite cements filling intergranular pore (PPL, well W159, 2572.15 m). (c) purplish red ferrocalcite cements filling intergranular pore and intragranular dissolution pore (PPL, well W30, 2666.2 m). (d) Ferrodolomite filling intergranular pore (SEM, well W25, 2601.9 m). (For interpretation of the references to color in this figure legend, the reader is referred to the Web version of this article.)



**Fig. 9.** Proportion of different clay minerals in Chang 8 reservoir.

rosette-like chlorite partially filling primary pore and secondary dissolution pore (Fig. 10c). Among the three morphologies pore-lining chlorite is the most common, which can exist alone or superimposed on the coated chlorite. According to the results of electron probe microanalysis (EPMA), the chlorite in the study area is rich in iron (Fig. 11).

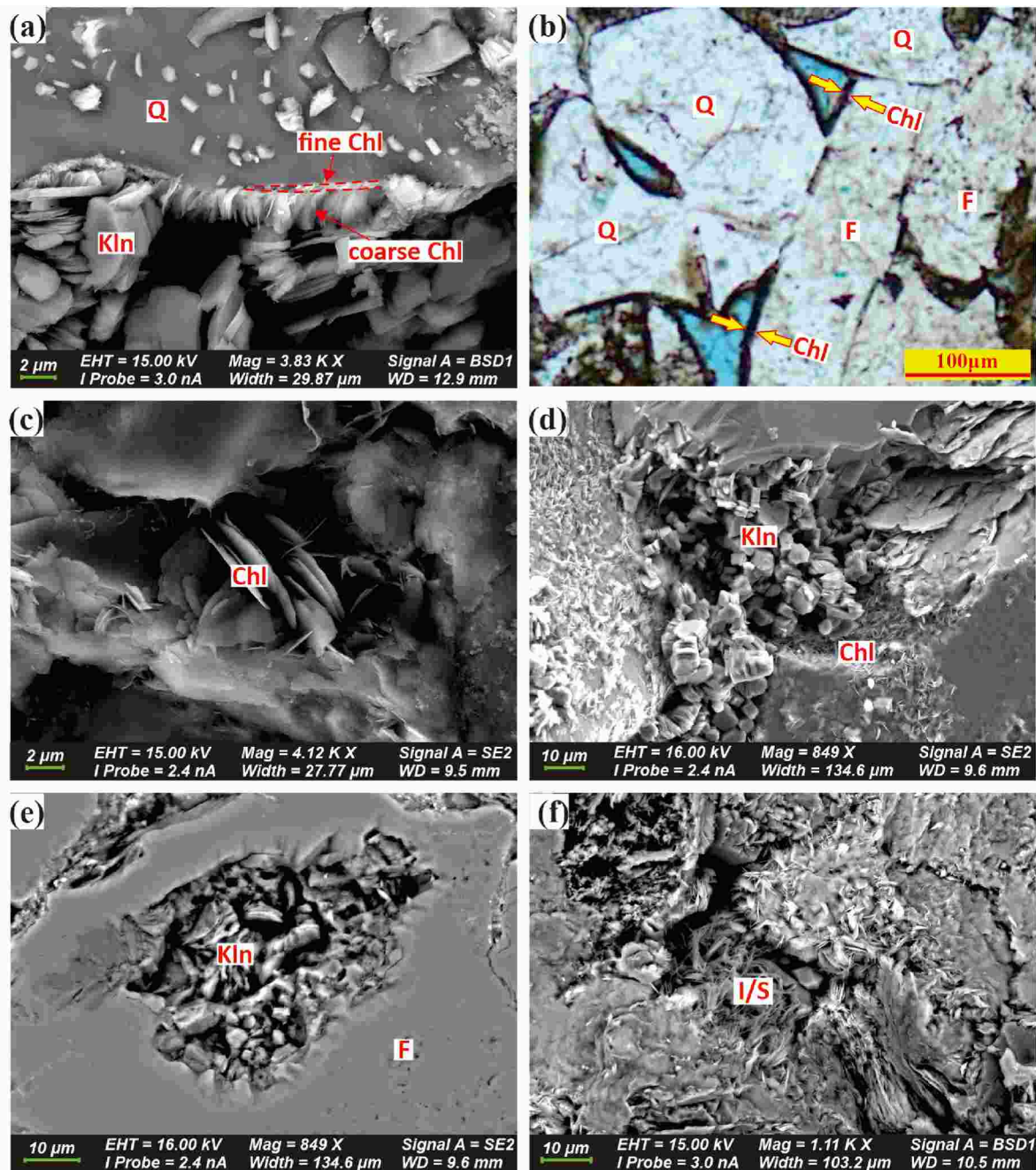
Authigenic kaolinite is the second most abundant clay mineral in Chang 8<sub>1</sub> oil-bearing, with proportion in the total content of clay minerals varies from 9% to 42% (avg. 18%). The authigenic single crystal of kaolinite is pseudo-hexagonal plates, while the aggregates are in the

form of book-like or vermicular stacks filling pores (Fig. 10d), and authigenic quartz is occasionally coexisted with them (Fig. 12a). The combination of individual kaolinite is relatively loose, thus a certain amount of intercrystalline micropores are often developed. The formation of kaolinite is closely tied to the dissolution of feldspar, and kaolinite is well developed in the place where feldspar strongly dissolved (Fig. 10e).

I/S mixed layer constitutes 12%–30% of the total clay minerals, with an average of 19.9%. I/S often appears in the form of lining cement on the surface of detrital grains, occasionally in the form of pore filling, and partially transformed into flaky illite (Fig. 10f). Authigenic illite accounts for 3%–22% of the total clay minerals (avg. 9.2%) and appears around the surface of detrital grains or irregular flaky in the intergranular pores, but rarely grows in the form of bridging.

**4.3.2.3. Siliceous cementation.** Siliceous cementation is another common cementation besides carbonate cements, and its volume fraction ranges from 15% to 20%, with an average of 17%. Siliceous cementation occurs in the form of authigenic quartz and quartz overgrowth, of which the former is relatively developed closely related to strong compaction and dissolution. The strong compaction and early carbonate cementation greatly reduced the intergranular volume, so that there was not enough space for quartz to grow along the surface of detrital quartz grains. The authigenic euhedral quartz crystals usually precipitated after strong compaction, distributing as hexagonal columns in intergranular pores and partial intragranular dissolution pores, perpendicular to detrital grains (Fig. 12b). In addition, euhedral quartz crystals are often associated with other diagenetic minerals, such as chlorite, kaolinite, I/S





**Fig. 10.** Micrographs showing microscopic characteristics of authigenic clay mineral cements in Chang 8 tight reservoir. (a) pore-lining chlorite growing perpendicular to detrital grain surface (SEM, well W42, 2668.17 m). (b) pore-lining chlorite on the surface of detrital grains at the edge of pores and undeveloped pore-lining chlorite at the grains contact (PPL, well W30, 2654.9 m). (c) rosette-like chlorite filling primary pore space (SEM, well W117, 2517.7 m). (d) book-like authigenic kaolinite crystals filling intergranular pore (SEM, well N248, 2447.9 m). (e) authigenic kaolinite filling intragranular pore of dissolved feldspar (BSE, well N168, 2483.2 m). (f) irregular flaky I/S mixed layer growing along the grain surface and filling intergranular pore (SEM, well W117, 2517.7 m).

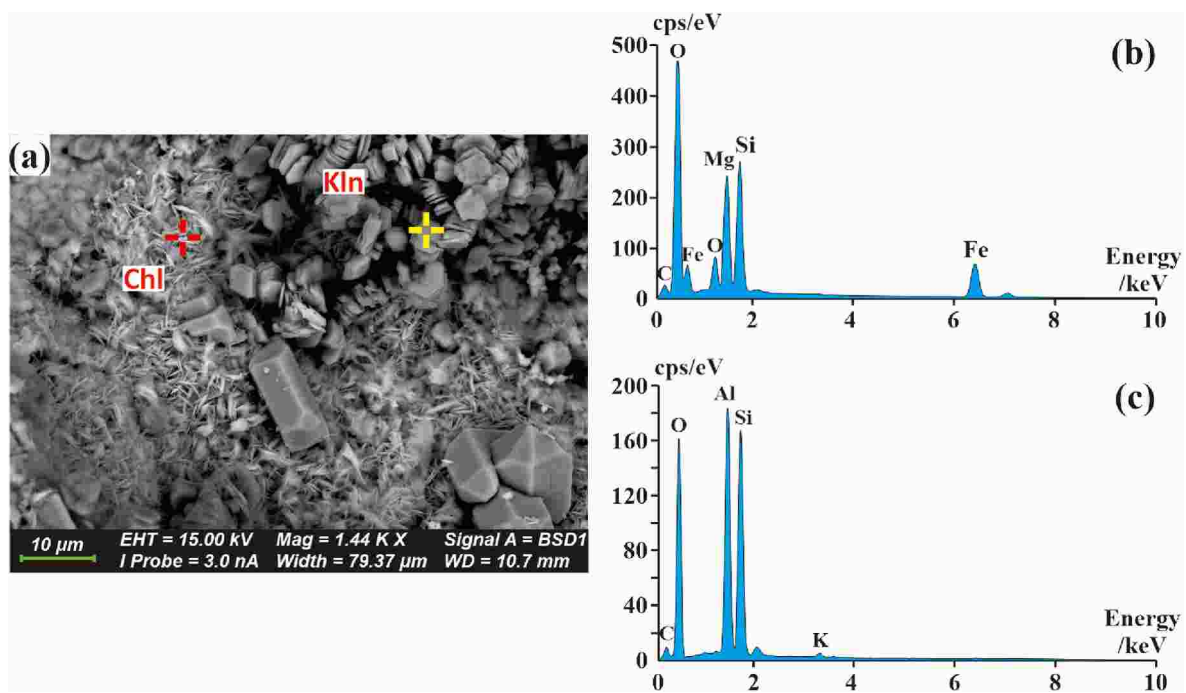
mixed layer and ferrocalsite (Fig. 12a and c). By means of casting thin sections, images of SEM and BSE, it is believed that widely developed siliceous cements in the study area not only filled the pores, but also blocked the throat, resulting in the destruction of petrophysics ultimately.

#### 4.3.3. Hydrocarbon emplacement and dissolution

The observation of cores and casting thin sections of Chang 8<sub>1</sub> tight sandstones shows that oil stains which probably came from the overlying source rock of Chang 7 member are developed in some wells (Fig. 12d), indicating the existence of hydrocarbon emplacement. The effects of hydrocarbon emplacement on reservoir are reflected in two

aspects (Nedkvitne et al., 1993; Higgs et al., 2007; Neveux et al., 2014): (i) fluids containing large amounts of organic acids enter the pore system, which changes the geochemical environment of rocks and the wettability of formation water, inhibiting quartz overgrowth and formation of authigenic illite in the inorganic diagenetic environment, thus weakening the mechanical diagenesis and chemical diagenesis. (ii) The unstable components such as feldspar are easy to be dissolved in acidic fluid environment, that is, hydrocarbon emplacement promotes the occurrence of dissolution.

As acidic fluids flow into the pore system of the reservoir, the unstable components are usually dissolved and then mixed intergranular pores as well as intragranular dissolution pores formed (Chen et al.,



**Fig. 11.** Micrographs illustrating the characteristics of authigenic chlorite and kaolinite: (a) microscopic morphology under BSE (Well N248, 2447.9 m). (b) EDS analysis of the point marked by the red cross in Fig. 11a. (c) EDS analysis of the point marked by the yellow cross in Fig. 11a. (For interpretation of the references to color in this figure legend, the reader is referred to the Web version of this article.)

2017; Liu et al., 2020). The observation of casting thin sections and SEM micrographs shows that the dissolution of detrital feldspar is generally most evident among unstable components (Fig. 12e), while the dissolution of rock fragments is rare. The dissolution of feldspar occurred in two ways: on the one hand, acid fluid flowed into the residual intergranular pores, dissolving the edge of detrital feldspar, thus forming mixed intergranular pores. On the other hand, acid fluid selectively dissolved feldspar along cleavage cracks, forming faveolate intragranular dissolution pores and occasionally moldic pores (in the case of complete dissolution of detrital feldspar) (Fig. 12f). Due to hydrocarbon emplacement and relatively strong dissolution in the study area, together with well-developed intergranular and intragranular dissolution pores, a reservoir with partially relatively high permeability (sweet spot) under the background of regional low permeability thus formed.

#### 4.4. Diagenetic sequence and stages

For purpose of ascertaining current diagenetic stage and the relative timing and duration of major diagenetic process in the Chang 8<sub>1</sub> reservoir, characteristics of authigenic minerals, organic maturity, paleo-geotherm, burial history curve and homogenization temperature (Th) of fluid inclusions were figured out in this study. As Chang 8<sub>1</sub> oil-bearing interval is adjacent to and below the source rock of Chang 7 member, the core analysis results of Chang 8<sub>1</sub> reservoir show that the vitrinite reflectance (Ro) of representative mudstone samples ranges from 0.62% to 1.25% (avg. 0.95%), and the homogenization temperature in quartz and carbonate cements is mainly distributed between 60 °C to 70 °C and 100 °C–130 °C (Fig. 13). In conclusion, the Chang 8<sub>1</sub> sandstones have experienced three incremental stages of diagenetic evolution, successively Eodiagenesis A, Eodiagenesis B and present Mesodiagenesis A, referring to the Chinese standard for classification schemes of sandstone diagenesis “SY/T5477-2003” (Yue et al., 2018).

It is difficult to determine the exact occurrence and duration of all diagenetic processes in those sandstones which have undergone complicated diagenetic alteration since buried. Nevertheless, the contacts and sequence of representative diagenetic minerals are identified

by means of casting thin sections, SEM and BSE images, and the diagenetic sequence has been summarized in Fig. 14:

- (i) Point contact is more common between the particles of sandstone cemented mainly by calcite, suggesting that calcite cementation may coexist with early compaction.
- (ii) Authigenic kaolinite fills intergranular pores with chlorite lining, and occasionally filled with intragranular dissolved pores of feldspar, suggesting that authigenic kaolinite was formed later than chlorite lining and feldspar dissolution.
- (iii) Authigenic quartz crystals are distributed on the surface of chlorite lining, indicating that its formation time is later than chlorite lining.
- (iv) Fe-calcite can be seen filling dissolution pore of feldspar, indicating that its formation is not earlier than that of feldspar dissolution.
- (v) I/S mixed layer grows on the surface of chlorite lining, which indicates that its formation is later than chlorite.

## 5. Discussion

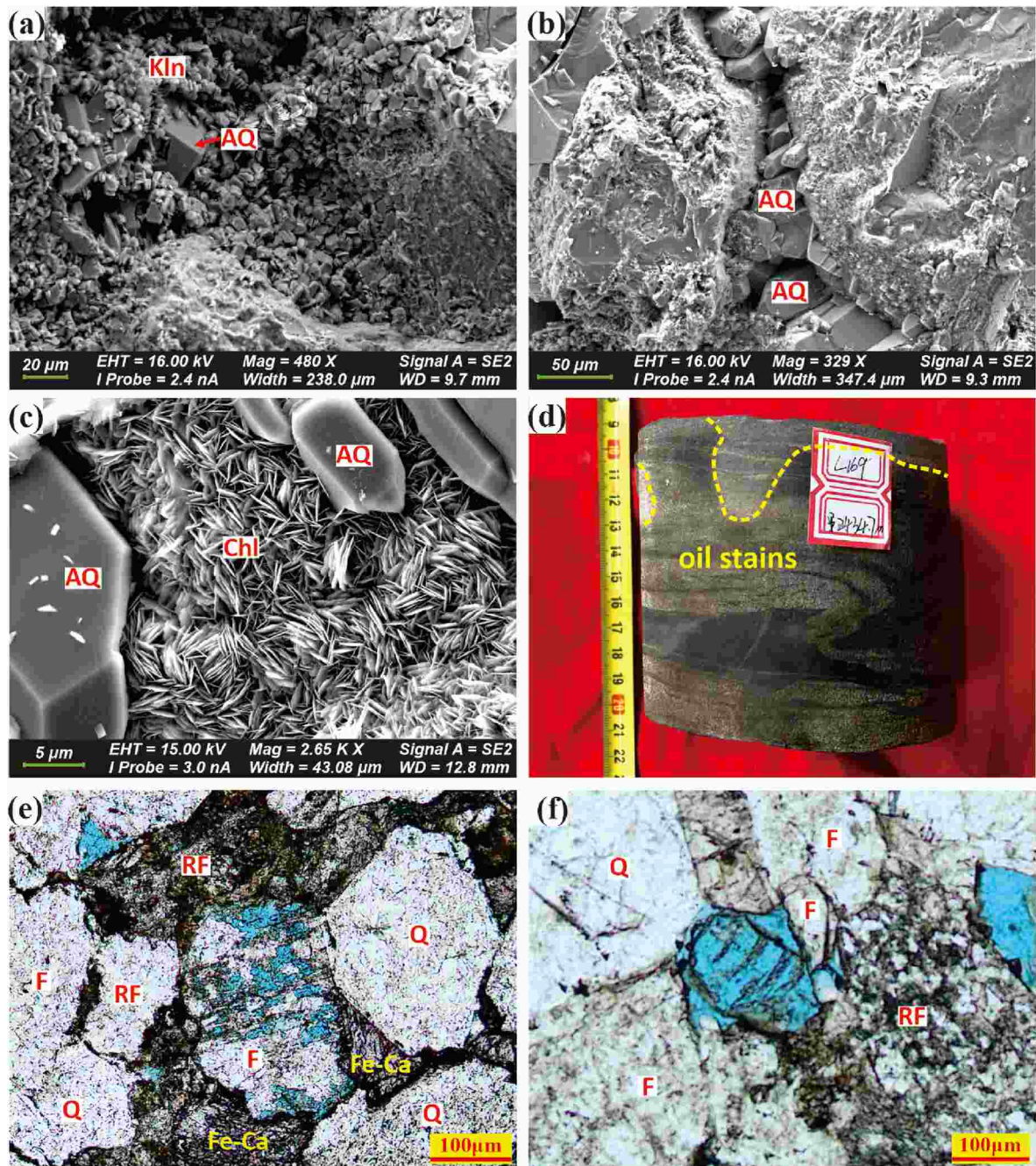
### 5.1. Main factors controlling reservoir quality of tight reservoirs

#### 5.1.1. Depositional settings and lithofacies

Found impacts of macro sedimentary settings on reservoir quality, which is mainly manifested in deposits and lithofacies. Taking well W105 as an example, there are certain differences in petrophysics among different deposits and lithofacies (Fig. 15). The petrophysical values of lithofacies iv or levee deposit are generally low, while the values of distributary channel or lithofacies i sandstones can be large or as small as lithofacies iv sandstones. As a whole the statistical results of petrophysics based on lithofacies classification in Chang 8 reservoir reveal that the reservoir quality of different deposits and lithofacies in digitate shallow-water lacustrine delta deposits shows certain regularity (Fig. 16).

Depositional settings and lithofacies are the basis for the formation of





**Fig. 12.** Micrographs showing microscopic characteristics of siliceous cements and dissolution in Chang 8 tight reservoir. (a) authigenic kaolinite coexisted with authigenic quartz crystals distributed in intergranular pore (SEM, well N248, 2447.9 m). (b) authigenic quartz crystals growing perpendicular to the surface of detrital grains (SEM, well N248, 2447.9 m). (c) scattered authigenic quartz distributed on pore-lining chlorite (SEM, well W42, 2668.17 m). (d) Visible oil stains in core sample (well N169, 2434.7 m). (e) dissolution pore in feldspar grain (PPL, well N169, 2460.1 m). (f) moldic pore formed by complete dissolution of feldspar grain (PPL, well N168, 2222 m).

various reservoir quality. Sandstones of lithofacies i deposited relatively in higher energy environment (distributary channel) are featured by the coarsest grain size, relatively good sorting, low content of matrix and ductile components, corresponding to the best reservoir petrophysics generally. In contrast, the sandstones of lithofacies iv which developed in low energy environment (levee) are finest-grained, poorly sorted with high content of matrix and ductile components among varied lithofacies, and the reservoir quality is the worst in the mass. Regardless of the difference of reservoir quality among deposits and lithofacies, reservoir quality equally varies as well in different locations of specific lithofacies, which is closely related to diagenetic type and intensity encountered by

sediments after deposited.

For example, when the distributary channel appears in upper delta plain, its bottom is often highly calcareous cemented to form very low petrophysics. As a contrast, when the distributary channel appears in the form of bar finger in the lower plain and front of the delta, the degree of calcareous bonding at the bottom is much lower (© in Fig. 6b). This is significantly different from other types of bird-foot delta (Ma et al., 2012; Li et al., 2017). The reason may be the influence of bounding surface between different deposits (or “architectural bounding surface”), which will be described later.

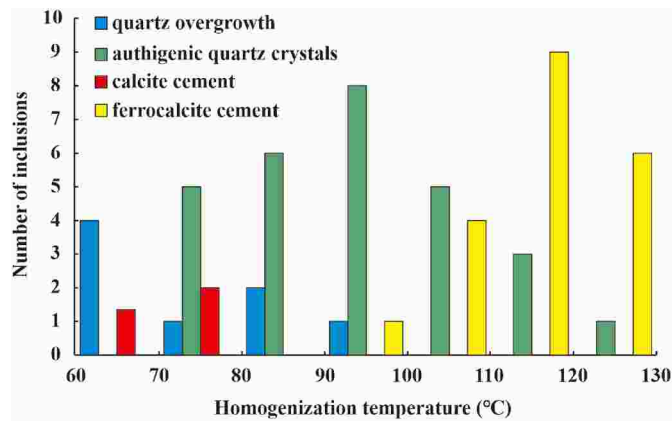


Fig. 13. Histogram showing the distribution of homogenization temperature of fluid inclusions.

### 5.1.2. Control of diagenetic alteration difference on reservoir quality

**5.1.2.1. Mechanical compaction.** Mechanical compaction loses the largest proportion of original pore space. Chang 8 member has experienced early rapid subsidence and continuous compaction after deposited, resulting in a great loss of original pore space and a sharp decrease in original petrophysics. The most important factor for the deterioration of petrophysics is the original depositional fabric of sandstones. In the case of the similar roundness of mineral particles in the study area, the influence of grain size, sorting, especially the content of ductile components and matrix on compaction is particularly important.

Most previous achievements have revealed that the proportion of ductile components is significantly positively correlated with the strength of compaction (Loucks et al., 1984; Trendell et al., 2012; Rossi and Alaminos, 2014; Henares et al., 2016). In other words, sandstones with high content of ductile components are not able to resist compaction, hence experienced more severe compaction. The content of ductile components (biotite, muscovite, soft rock fragments such as mudstone, phyllite, schist and extrusive rocks) in Chang 8 reservoir varies greatly, ranging from 4% to 45%, with an average of 29%. As is shown in the scatter plot of the content of ductile components and compactional porosity loss (COPL) (Fig. 17), with the increase of the content of ductile

components, the COPL tends to increase, and the COPL differs among different lithofacies. According to the scatter plot of COPL and cementational porosity loss (CEPL) (Fig. 18), the sandstones of coarser-grained lithofacies i and lithofacies ii with lower content of ductile components show COPL of 23% and 27% respectively, which is significantly lower than that of finer-grained lithofacies iii and iv with high content of ductile components (avg. 33% and 36%, respectively). It should be noted that the early calcite cementation degree and compactional strength in the study area often fluctuate in turn, and meanwhile the development of chlorite also inhibits the compaction to some extent. The COPL of partial coarse-grained sandstones slightly decreases due to the development of early carbonate cements or pore-lining chlorite (Figs. 8 and 10).

**5.1.2.2. Carbonate cementation.** As mentioned above, as the most common carbonate cements in Chang 8 sandstones, calcite and ferrocalcite mainly filled primary and secondary dissolution pore space. Previous studies reveal a significant negative correlation between reservoir petrophysics and carbonate content when the content of carbonate in sandstones reaches a certain proportion (Zhou et al., 2016; Wang et al., 2020). In Chang 8 sandstones of Maling Oilfield, the maximum value of reservoir petrophysics decrease obviously when the carbonate content occupies more than 10% of the total volume (Fig. 19). Therefore, considering the widespread development of carbonate cements in the study area, their serious damage to reservoir quality should be focused on.

Carbonate cementation mainly blocks the pores of coarser sandstones. The occurrence of carbonate cementation is closely related to the architecture of sand bodies and depositional fabric, both of which can be reflected in deposits and lithofacies. The top and bottom of thicker, well sorted and coarser sand bodies, i.e., the top and bottom of channels in the upper plain, and the top of channel of bar fingers in the lower plain and front of the delta, which correspond to lithofacies i or ii, are often the main sites for the occurrence of carbonate cementation. When the thickness of sand bodies is obviously less than 1 m, some fine-grained sandstones and coarse siltstone may also be cemented. In addition, weak cementation is sometimes observed at the bottom of the distributary channel of bar fingers in lithofacies i, which may be related to the architectural bounding surface and the widely distributed intergranular pores and secondary dissolution pores here. Taking well W105 as an example (Fig. 15), well-developed calcareous cementation is common at

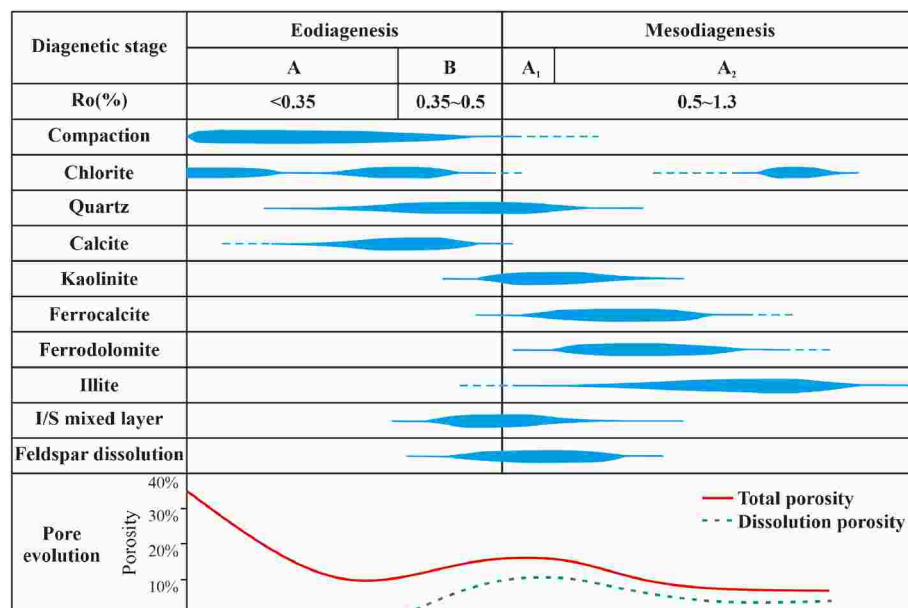


Fig. 14. Diagenetic evolution sequence and pore evolution history of Chang 8 tight reservoir in Maling Oilfield.



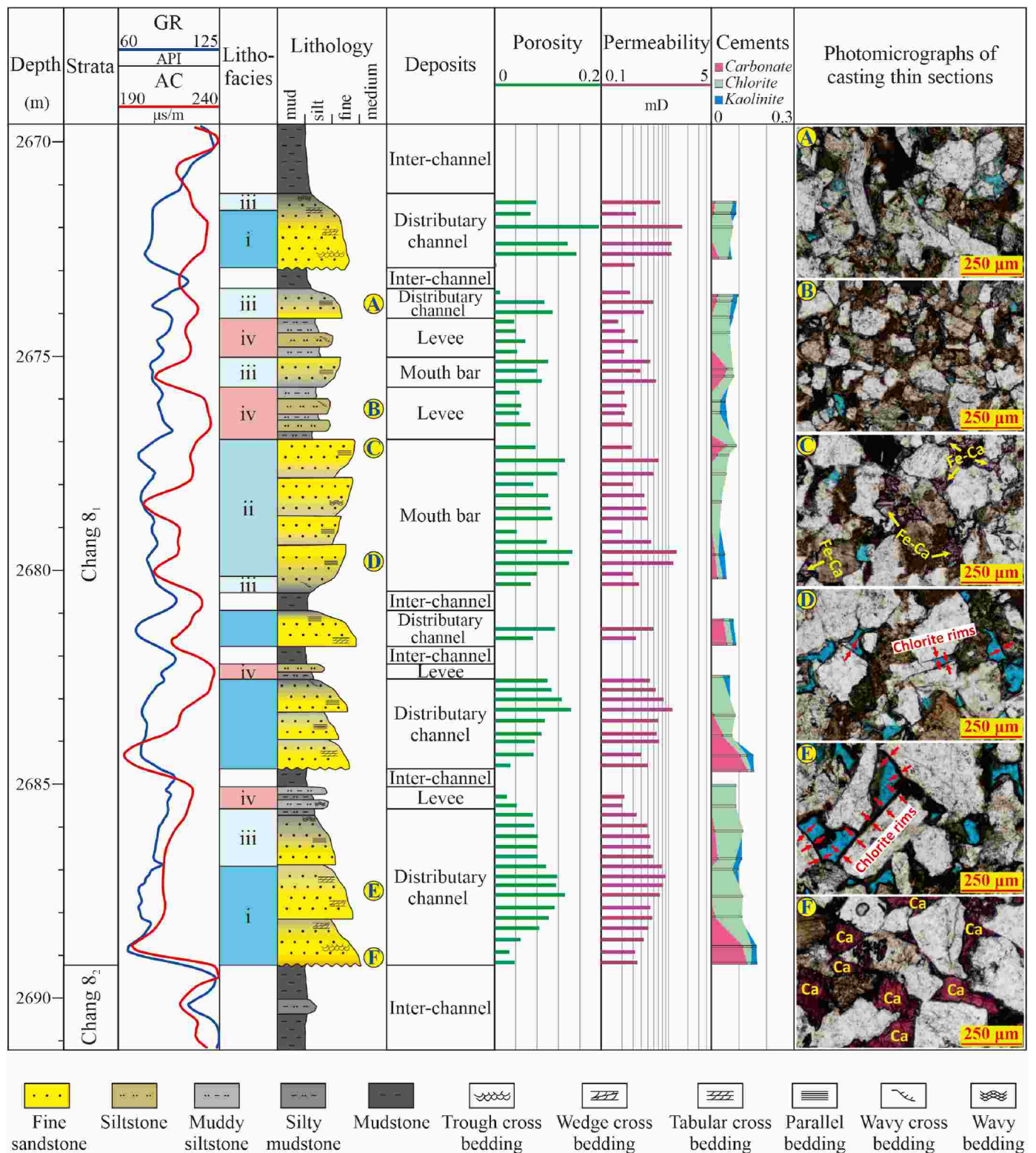


Fig. 15. Stratigraphic column of well W105 showing the vertical distribution of petrophysics and the contents of primary diagenetic minerals.

the top and bottom of thick sand bodies during 2685.6 m–2689.1 m (with a volume of 5%–25%), while the internal cementation of sand bodies is obviously rare (with a volume of 1%–5%). In addition, there is moderate content of carbonate cements at the top of fine-grained mouth bar sandstones between 2676.8 m and 2677.3 m. The distribution of carbonate cements in sandstones indicates that their precipitation may be relevant to the adjacent dense mudstone.

The statistical results state clearly that the content of carbonate cements is related to the distance from sandstone-mudstone interface, which is also reflected in the divergence of reservoir quality (Fig. 20). When the distance between broken sandstone sample and the adjacent sandstone-mudstone interface is less than 1 m, the carbonate content of sandstone is up to 27% for lithofacies i, with an average of 15%. However, when the sample point is located at the middle of the sand body



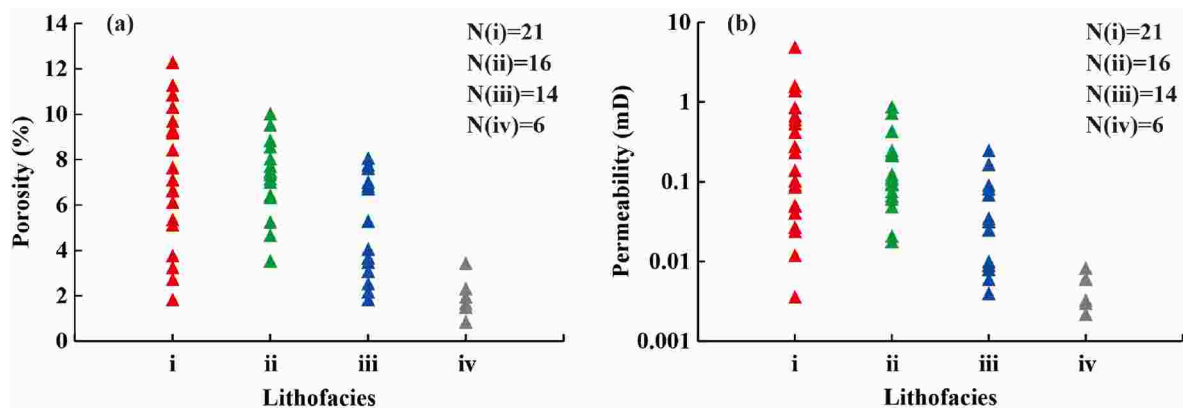


Fig. 16. Cross plot showing the relationship between the lithofacies and the (a) porosity, (b) permeability.

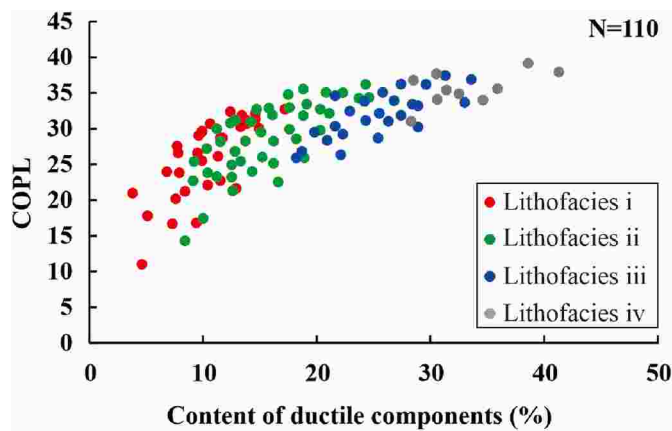


Fig. 17. The correlation between the content of ductile components and compactional porosity loss (COPL).

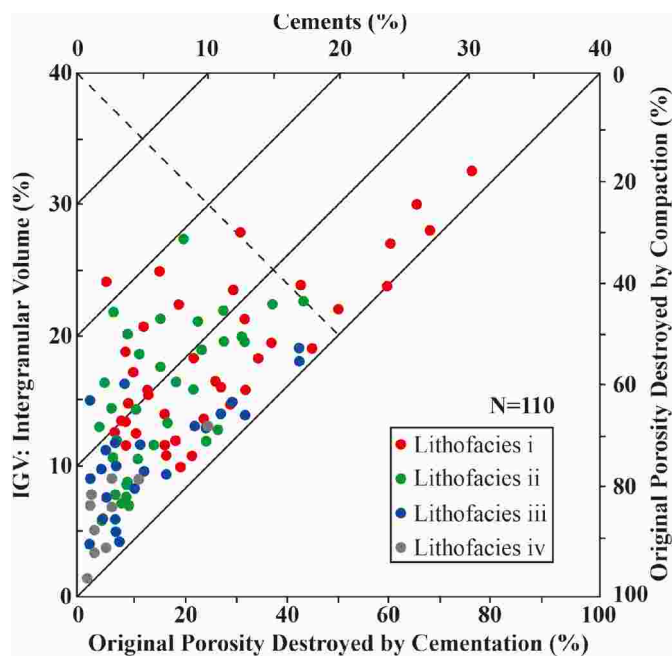


Fig. 18. Cross plot showing the relative importance of mechanical compaction versus cementation on the loss of original intergranular volume (diagram corrected after Ehrenberg, 1989).

and is more than 1 m away from the interface, the content of carbonate cements decreased rapidly, and occupied less than 10%, with an average of 5%. In addition, low values of carbonate cements can occur at different distances from the sandstone-mudstone interface, probably due to the difference among lithofacies. For example, even if the distance from sandstone-mudstone interface is less than 1 m, the maximum content of carbonate cement of lithofacies iv sandstones is no more than 5% because there is almost no pore space for cementation. As a comparison, for sandstones of lithofacies i, the content of carbonate cements less than 5% is common only when the distance is more than 1 m away from sandstone-mudstone interface.

Since no detrital carbonate particles are found in Chang 8 tight sandstones, it is suggested that the calcium ions, iron ions and magnesium ions necessary for carbonate cementation are not originated from detrital carbonate particles, but most likely from adjacent mudstone. Previous studies pointed out that these ions can be released from the dissolution of feldspar in mudstone, the formation and transformation of clay minerals, as well as the maturation of organic matter (Chowdhury and Noble, 1996; McHargue and Price, 1982; Dutton, 2008). The similar carbon isotopic compositions of sandstone and mudstone indicate that these ions and carbon dioxide in sandstone cements most possibly came from adjacent mudstone (Table 2). These ions were released by mechanical compaction and subsequent hydrocarbon generation pressurization during the burial process of mudstone, then flowed into adjacent pore space of the sandstone, and precipitated when the pressure decreased.

Furthermore, the distribution of carbon isotope in cements reflects its sources, organic or inorganic. Compared with inorganic (atmospheric) carbon, the carbon isotope distribution of organic carbon is lighter than that of inorganic carbon (about  $-18\text{‰}$ – $-33\text{‰}$  and  $-7\text{‰}$ , respectively) (Melezhik et al., 2003; Woo and Khim, 2006), that is, the lighter carbon isotope reflects the decrease of the proportion of organic carbon source in sediments. The carbon isotope of calcite cement in Chang 8 formation is mainly distributed in  $-1.5\text{‰}$ – $-2.0\text{‰}$ , with an average of  $-0.6\text{‰}$ , which indicates that the source of early carbonate cementation is mainly inorganic, consistent with the homogenization temperature distribution of inclusions. The homogenization temperature of calcite measured by fluid inclusions is generally about  $80\text{ }^{\circ}\text{C}$ , indicating that the strata studied had not entered the deep burial stage and the compaction had not occurred extensively during the formation of calcite. The carbonate cements of ferrocalcite and ferrodolomite mainly filled intergranular pores and partial dissolution pores, and their carbon isotopes are obviously lighter, ranging from  $-5.2\text{‰}$  to  $-3.6\text{‰}$  (with an average of  $-4.5\text{‰}$ ), reflecting the increase of organic source components during the cementation of these carbonates. The inclusions show that the homogenization temperature of these two types of carbonate cements is higher ( $110\text{ }^{\circ}\text{C}$ – $120\text{ }^{\circ}\text{C}$ ), and the ferrocalcite cements seen filling the feldspar dissolution pore indicates that the earlier or

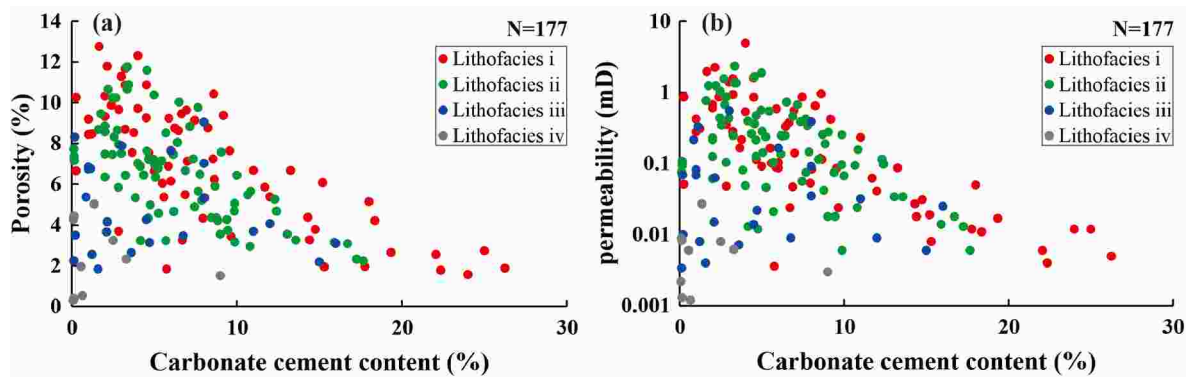


Fig. 19. The relationship between the absolute proportion of carbonate cements (CCC) and petrophysics: cross plots of CCC vs (a) porosity and (b) permeability.

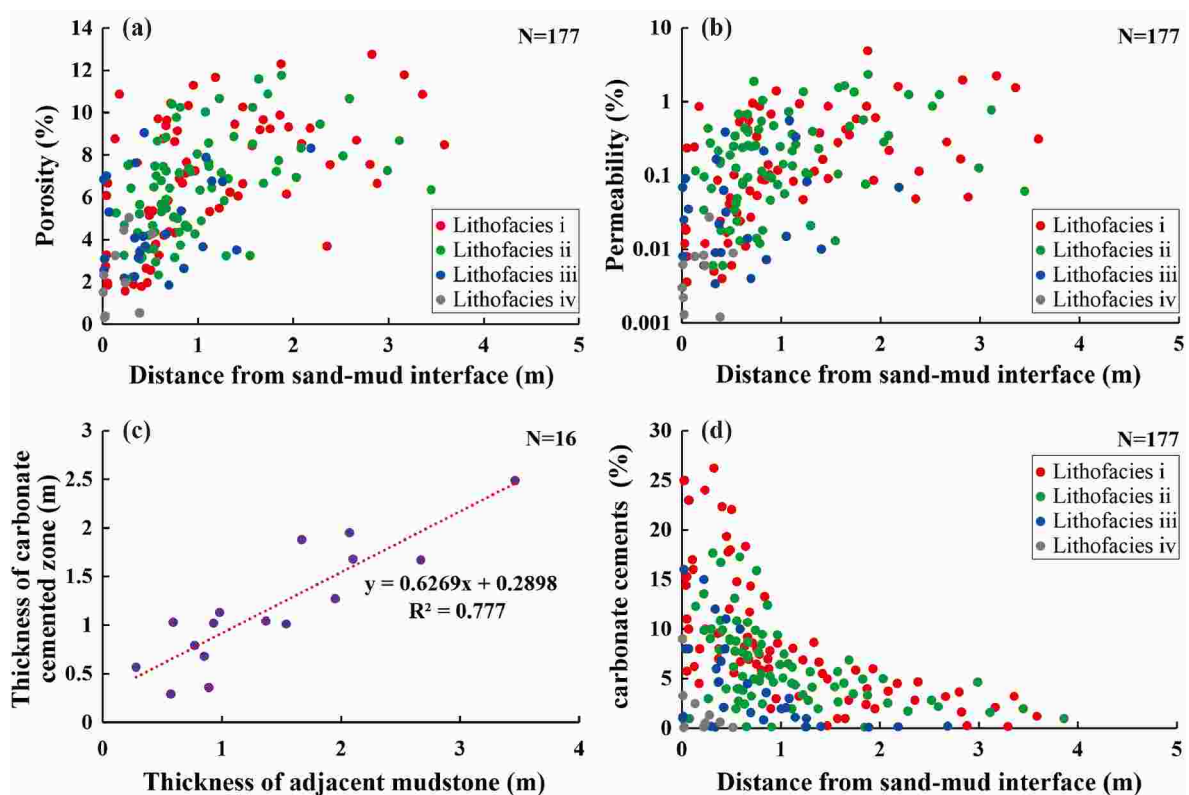


Fig. 20. The cross plots showing the correlations among related parameters of carbonate cemented sandstones and reservoir petrophysics: the relationship between (a) the distance from the adjacent sandstone-mudstone interface (DSMI) and the porosity, (b) DSMI and the permeability, and (c) the thickness of adjacent mudstones and the thickness of carbonate cemented zones. (d) DSMI and CCC in sandstones.

simultaneous dissolution of feldspar may provided  $\text{CO}_3^{2-}$  for their cementation (Fig. 8c).

There are more primary and secondary pore space in coarser sandstones, consequently more carbonate cements precipitated in the pores of these sandstones adjacent to the mudstone, which also explains why this cementation phenomenon is more developed particularly at the top and bottom of sandstones related to lithofacies i and lithofacies ii. As mentioned above, the dissolution of detrital feldspar particles and the transformation of clay minerals in sandstones also release a small amount of ions and carbon dioxide, which is an important reason why weak carbonate cementation occasionally occurs at the bottom of fine-grained lithofacies ii sandstones located at the bottom of channels of bar fingers in delta front that far away from the sandstone-mudstone interface.

**5.1.2.3. Chlorite cementation.** Chlorite is the most common cement among all types of clay minerals cementation, and mainly grew perpendicular to the surface of detrital grains and wrapped the grains in the form of pore-lining. While the content of rosette-like chlorite filling pore space is rare, and the chlorite coatings are hard to observe in SEM and BSE images since it's extremely thin and wrapped by pore-lining chlorite. Therefore, these two types of chlorite cements are not discussed in detail in this study. Previous scholars have done much research on the precipitation sources of chlorite, including the alteration of early chlorite, the recrystallization of montmorillonite in the transformation process of mixed layer I/S, dissolution and reprecipitation of lithic fragments of volcanic rock, and redistribution of early chlorite coatings based on Ostwald process (Jahren, 1991; Hillier, 1994; Aagaard et al., 2000; Grigsby, 2001; Gould et al., 2010). Among various precipitation sources, the abundant Fe ion would favours chlorite. Combined with the development history of Ordos Basin, it is considered that the Fe element

**Table 2**

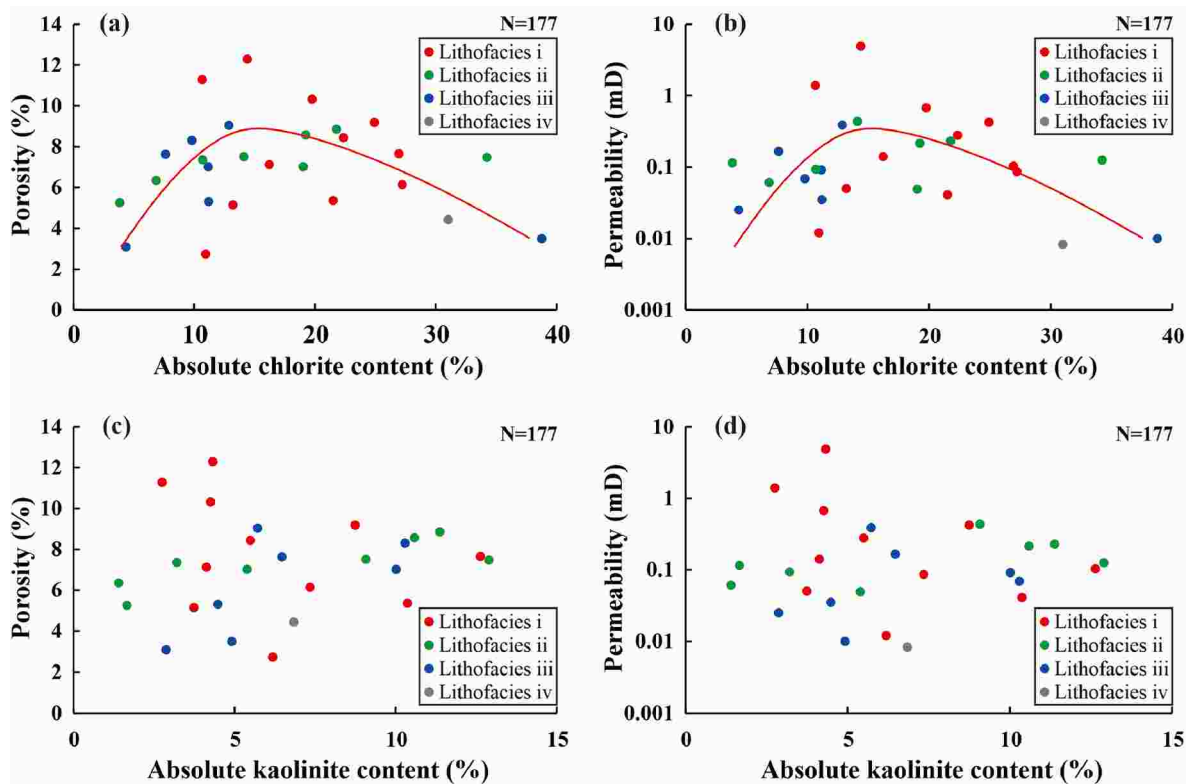
Compositions of carbon and oxygen isotopes of mudstones and carbonate cements in Chang 8 formation.

Well	Depth (m)	Lithology	Carbonate cement type	Occurrences	$\delta^{13}\text{C}_{\text{PDB}}/\text{‰}$	$\delta^{18}\text{O}_{\text{PDB}}/\text{‰}$
W30	2663.7	Fine sandstone	Ferro-calcite	Bottom of channel	-5	-18.9
N168	2492.3	Medium sandstone	Calcite	Bottom of channel	-1.3	-16.9
N216	2548.2	Fine sandstone	Calcite	Top of channel	1.7	-17.5
N216	2554.1	Medium sandstone	Calcite	Bottom of channel	-0.8	-15.3
W159	2571.5	Fine sandstone	Calcite/Ferro-calcite	Bottom of channel	-3.7	-16.6
W159	2574.9	Siltstone	Ferro-calcite	Natural levee	-4.7	-22.8
W105	2673.1	Fine sandstone	Calcite/Ferro-calcite	Bottom of channel	-3.5	-21
W105	2689.6	Medium sandstone	Calcite	Bottom of channel	-1.4	-15.9
W30	2663.9	Mudstone	-	Interdistributary bay	-2.1	-20.3
N168	2492.8	Mudstone	-	Interdistributary bay	0.6	-18.7
N216	2546.4	Mudstone	-	Interdistributary bay	-1.4	-16.7
N216	2554.9	Mudstone	-	Interdistributary bay	-4.2	-19.8
W159	2570.8	Mudstone	-	Muddy intercalation	-3.9	-17.4
W159	2572.6	Mudstone	-	Interdistributary bay	-4.1	-18.8
W105	2670.2	Mudstone	-	Interdistributary bay	-2.1	-17.7
W105	2690.2	Mudstone	-	Interdistributary bay	-0.5	-17.5

may mainly come from the weathered volcanic rock debris from western Liupan Mountain. The deposition Fe in the volcanic rock debris was injected into the salty lacustrine water along with the river system to form flocculation Fe, which was then dissolved into Fe ions and entered the formation water. Moreover, feldspar dissolution also released a small amount of Fe, Mg, Al and Si ions into formation water to form authigenic chlorite.

Pore-lining chlorite mainly developed in relatively coarser-grained sandstones corresponding to lithofacies i and lithofacies ii, according to the observation of casting thin sections and SEM micrographs (Fig. 10a and b). Sufficient pore space is a necessary condition for the crystals' growth of pore-lining chlorite, which is mainly controlled by compaction strength, early cementation degree and matrix content. During diagenesis, coarser-grained sandstones far from the sandstone-mudstone interface in lithofacies i and lithofacies ii underwent

moderate compaction and weak carbonate cementation, thus more pore space was retained (Fig. 7a), while lithofacies iii and lithofacies iv with higher ductile composition and higher matrix content underwent strong mechanical compaction (Fig. 7d). Therefore, in the narrower pores of strongly compacted sandstones of lithofacies iii and lithofacies iv, ions in formation water didn't tend to precipitate chlorite crystals due to high pore pressure, while the relatively lower pore pressure generated in larger pore space existing in the sandstones of lithofacies i and lithofacies ii is more favorable for the precipitation of chlorite crystals and growing perpendicular to the surface of parent detrital grains. Furthermore, carbonate cements (mainly calcite) developed earlier than authigenic chlorite are embedded between intergranular pores, blocking a large amount of primary pores and throats, which is not conducive to the inflow of formation water and the precipitation of pore-lining chlorite. Generally, pore-lining chlorite is more developed in medium-



**Fig. 21.** The cross plots showing the correlations between absolute content of different clay minerals and reservoir petrophysics. (a) chlorite vs porosity, (b) chlorite vs permeability, (c) kaolinite vs porosity, and (d) kaolinite vs permeability.



fine grained sandstones with clean pore space than fine-grained sandstones and siltstones with high matrix content and severe cementation, while the thickness of pore-lining chlorite in coarser-grained sandstones of lithofacies i is thicker than that of sandstones of lithofacies ii. This kind of iron-bearing chlorite cemented sandstones are mainly confined to high-energy hydrodynamic conditions, including distributary channels in the plain and most of the bar fingers in the front.

Chlorite cementation plays a dual role in pore evolution of tight reservoirs. The appearance of authigenic chlorite cements improved the reservoir quality to some extent, which can be seen from the scatter diagram of chlorite content and reservoir petrophysics (Fig. 21a and b). When the absolute proportion of chlorite is less than 15%, pore-lining chlorite on the detrital grain surface dominated, resisting the compaction and close contact of grains, which is conducive to retain the original pore space, and thus the reservoir petrophysics are positively correlated with the absolute proportion of chlorite. However, when the absolute content exceeds the threshold value of 15%, the petrophysics of chlorite get worse on the contrary because the overdeveloped chlorite blocked the throats and some small pore. Occasionally, pores with pore-lining chlorite developed along the grain surface are partly filled with authigenic quartz crystals or ferrocalcite precipitated in Mesodiagenesis (Figs. 8c and 12c). Therefore, only in the case that the space developed by pore-lining chlorite resisting compaction in sandstones was not filled by later authigenic diagenetic minerals, effective reservoirs with relatively high permeability would form under the background of overall low permeability.

**5.1.2.4. Kaolinite cementation.** Kaolinite is another kind of authigenic clay mineral which is second only to chlorite in Chang 8 reservoir, and its influence on reservoir quality is negative. Authigenic kaolinite is abundant in the pores with strong dissolution of feldspar, and most of them filled intragranular dissolution pores, followed by some intergranular pores, indicating that the formation of kaolinite in diagenetic stage is probably related to the dissolution of feldspar. Previous achievements have confirmed that the dissolution of feldspar by atmospheric fresh water and organic acids released aluminum and silicon ions. When pressure decreased and environment changed, these ions migrated with formation water and precipitated, forming authigenic kaolinite crystals ultimately. The occupation of pore space and the blockage of throats by kaolinite, together with complex bending micropores formed between single kaolinite crystals, usually lead to the reduction of effective storage space and reservoir petrophysics, but this destructive impact on pore space is limited (Fig. 21c and d).

**5.1.2.5. Dissolution.** Dissolution primarily expands the pore space of coarser sandstones. Microscopic observation shows that a few dissolution pores are developed, and the volume proportion of secondary dissolution pore is in the range of 2%–5%, with a relative proportion of 30% on average of total pore space, which improved the reservoir quality to a certain degree. Organic matter in overlying Chang 7 source rock released organic acid and carbon dioxide after maturity, which is discharged into Chang 8 sandstones due to hydrocarbon-generating pressurization, and formation water rich in organic acid flowed in pore and dissolved unstable particles dominated by feldspar to form secondary dissolution pore. In the strata studied, secondary dissolution pore is the most common in sandstones of lithofacies i in Chang 8 sandstones, followed by sandstones of lithofacies ii (Fig. 12e and f), and hardly developed in sandstones of lithofacies iii and lithofacies iv, indicating that the water-rock reaction occurred more frequently in sandstones with coarser grain and lower ductile composition (Li et al., 2017). However, the improvement of reservoir quality is limited due to relatively poor connectivity of secondary intragranular dissolution pores, unless dissolution occurred along the grain edge or formed moldic pore and the dissolution pore was not cemented by later carbonates and clay minerals.

### 5.1.3. Relationship between architectural bounding surface and diagenetic alteration

The architectural bounding surface exerts a considerable impact on reservoir petrophysics, which can also be reflected in shallow-water delta reservoirs (Zhang et al., 2021). In the upper plain of digitate shallow-water deltas in this study, the bounding surface between distributary channel and inter-channel is the main type of architectural bounding surface (Fig. 22a). coarse-grained sandstones of distributary channels around such bounding surface were strongly calcareous cemented (Fig. 19), due to direct contact with mudstone (mentioned earlier).

Nevertheless, when it comes to the bar fingers located in the lower plain and front of the delta, the influence of architectural bounding surface on the reservoir quality is not as obvious as that of the upper plain (Li et al., 2017). In the bar fingers, the distributary channel closely coexists with mouth bar and together extends to the distal lacustrine in a finger shape. At the bounding surface of these two architecture units, the degree of carbonate cementation is low, probably because it is far away from the mudstone that provides the source of cements (Fig. 19). Significantly, although the bar fingers are surrounded by inter-bar mudstone providing source of carbonate cements, it's difficult for a considerable amount of ions to flow and precipitate in limited pore space to form carbonate cements due to the finer grain of sandstones (coarse siltstones to fine-grained sandstones at the bottom of mouth bar and siltstones of natural levee at the top of bar fingers) in contact with mudstone at the architectural bounding surface, compared with the coarser sandstones of distributary channels in the upper plain of the delta. The finer-grained outer edge of the bar fingers also prevented the formation water carrying ions from flowing into the interior of bar fingers, in spite of internal coarser-grained sandstones. Therefore, the petrophysics at the bottom of the channel in the bar finger are obviously better than those of the sandstones at the bottom of the channel in the upper plain (Fig. 22b).

At the end of the bar finger in the delta front, channel and levee deposits terminate, while the mouth bar continues to advance for a short distance, and thus the top of the most front-end mouth bar deposit is in direct contact with the mudstone of inter-bar deposit. Therefore, relatively strong carbonate cementation generally occurred in the fine sandstones at the top of the mouth bar that near the architectural bounding surface here (Fig. 22c).

### 5.2. Summary of distribution and evolution patterns of diagenesis

As mentioned above, due to the differences among deposits and lithofacies, the intensity of diagenesis in Chang 8 tight reservoir differs. The diagenetic differences between the three main sand-prone deposits (distributary channel, mouth bar and natural levee, respectively) and lithofacies from the plain to front of the shallow-water lacustrine delta are summarized into five main evolution patterns, as shown in Fig. 23.

Pattern I mainly exists in the main part of distributary channels in the upper plain which is far away from the sandstone-mudstone interface, predominant in the sandstones of lithofacies i. The medium-fine grained sandstones deposited in high hydrodynamic conditions are featured by the coarsest grain size, better sorting, and the lowest contents of matrix and ductile components, thus forming larger original pore space. This kind of sandstones experienced moderate compaction, widely chlorite lining, weak or no carbonate cementation and strong feldspar dissolution after deposition. Since constructive diagenetic alterations are more developed than the destructive diagenetic alterations in these sandstones, most of the pore space, including intergranular pore and secondary dissolution pore, has been reserved, thus forming the best reservoir.

Pattern II exists in the main part of bar fingers (except for the levees and the top of the channels) in the lower plain and front of the delta, as well as the middle and lower part of mouth bar at the distal end of bar fingers (distributary channel and levee are not developed in this case),

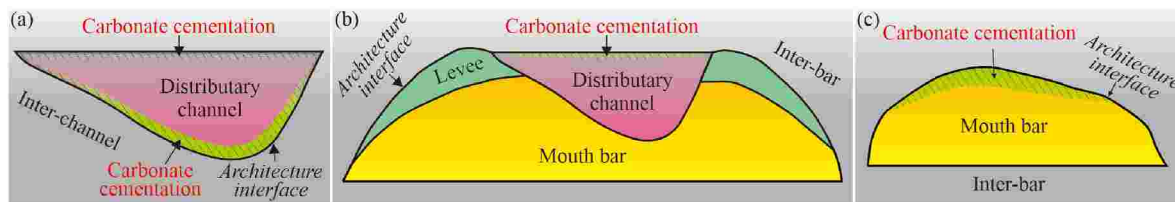


Fig. 22. Schematic diagram of cross section showing architecture units and carbonate cementation degree at different location on the plane of digitate shallow-water lacustrine delta: (a) distributary channel in the upper plain, (b) bar finger in the lower plain and delta front, (c) mouth bar at the end of the bar finger.

predominant in the sandstones of lithofacies ii. The hydrodynamic condition of these sandstones is relatively weaker than that of channels, and the fine-grained sandstones are usually moderately well sorted with low content of ductile components, forming relatively high original pore space. Sandstones of this pattern are characterized by moderate to relatively strong compaction, weak carbonate cementation, widely chlorite lining and moderate dissolution, thus most intergranular pores and a small number of intragranular dissolution pores are reserved eventually. Pattern II with relatively high petrophysics is the most widely developed diagenetic pattern.

Pattern III exists in the edge of channels, including distributary channel in proximal part and distributary channel of bar fingers in distal part of the delta, corresponding to sandstones of lithofacies iii. Due to the weak hydrodynamic condition at the edge of the channels, the sediments are finer in grain size and mainly consist of coarse siltstones and very fine-grained sandstones with moderate content of ductile components, forming moderate original pore space. Sandstones of this pattern experienced strong compaction, limited chlorite lining, moderate carbonate cementation and later weak dissolution after deposited. Only a few pores were partially retained, leading to relatively poor reservoir quality ultimately.

Pattern IV exists not only at the top and bottom of the channel in the upper plain and the top of channel of bar fingers in the lower plain-front of the delta, corresponding to lithofacies i or lithofacies ii, but also at the top of mouth bar of the distal end of bar fingers, corresponding to lithofacies ii. Although this kind of medium-fine grained sandstone has low content of matrix and ductile composition, even almost highest original pore space, it has experienced strong carbonate cementation in the process of burial diagenesis, including calcite cementation in Eodiagenesis period, ferrocalcite and ferridolomite cementation in Mesodiagenesis, due to the close proximity to the sandstone-mudstone interface. The extremely limited chlorite lining and weak dissolution in the later stage seriously limited improvement on the reservoir quality, resulting in a sharp drop in the original porosity, so that almost no pore space was retained. This pattern is also common since sandstones of lithofacies i and ii are prevalent in the study area.

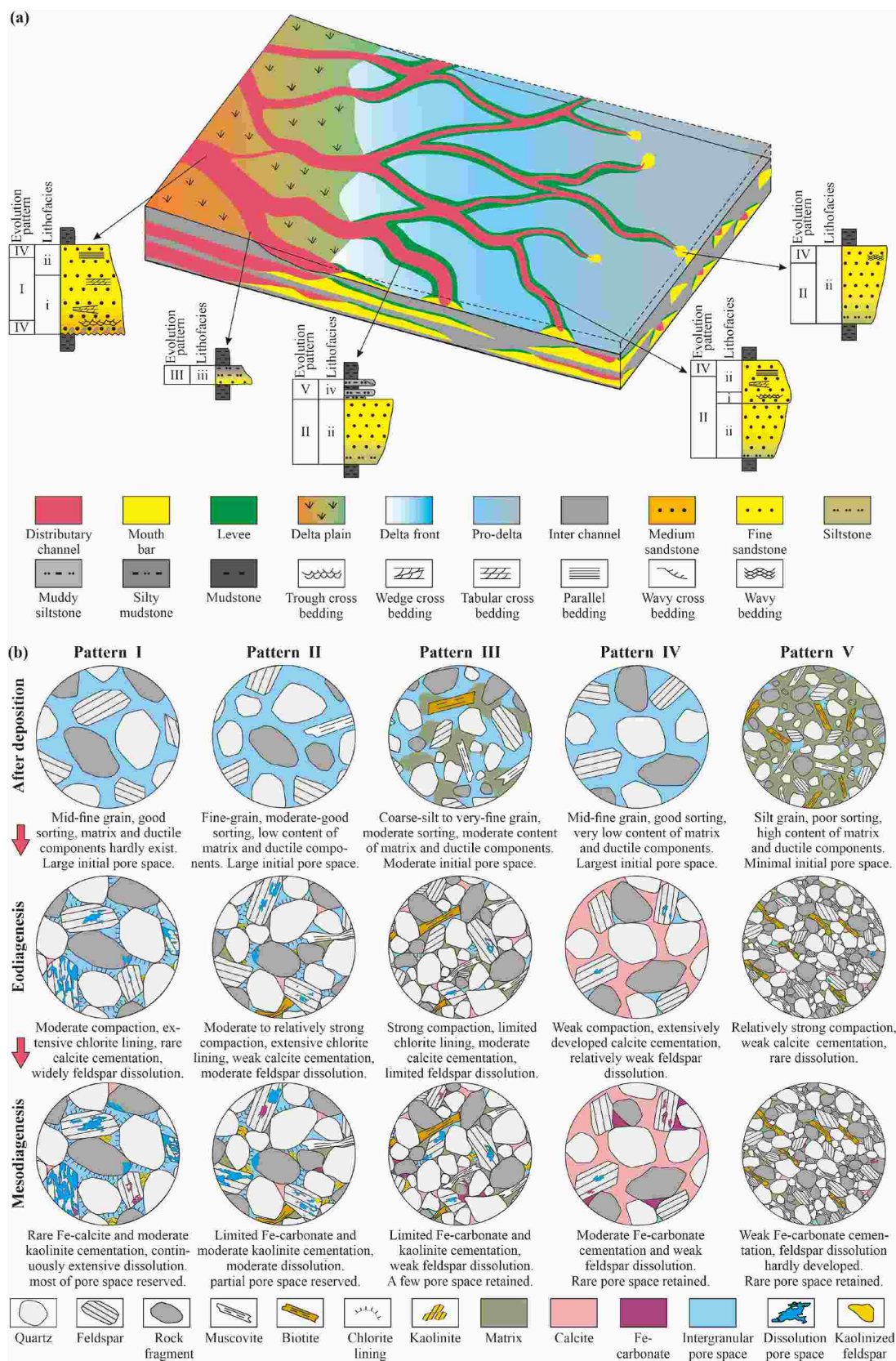
Pattern V occurs in the siltstone of levee and is related to lithofacies iv. This kind of siltstone with the smallest grain size, the highest content of ductile components and small original pore space experienced diagenetic alteration characterized by strong compaction during burial, accompanied by weak carbonate cementation and limited chlorite cementation, and the late dissolution was hardly developed. The reservoir quality of pattern IV and pattern V is the worst, which is not regarded as effective reservoir for hydrocarbon exploration and development.

## 6. Conclusions

- (1) Digitate shallow-water lacustrine delta deposits developed in Chang 8 reservoir of Maling area, and distributary channel, mouth bar, natural levee and interdistributary bay are the four main types of deposits. The sand bodies are mainly single distributary channel in upper delta plain, and digitate compound sand body in the lower plain and front of the delta, namely, bar

fingers, which composed of distributary channel corroding the mouth bar and levees on both sides of the channel, extending into the shallow lake in a finger shape. In addition, four types of lithofacies were identified in digitate shallow-water lacustrine delta of Chang 8<sub>1</sub> tight reservoir in the study area, considering the grain size, depositional structures and content of ductile components, successively lithofacies i, ii, iii and iv. Lithofacies i is chiefly medium-fine grained sandstones with cross bedding or parallel bedding developed, and it has extremely low content of ductile components. Lithofacies ii refers to fine-grained sandstones with wavy bedding or massive structure, and the proportion of ductile components is relatively low. Lithofacies iii represents coarse siltstones to fine-grained sandstones with moderate content of ductile components developed at the edge of the distributary channel, while lithofacies iv generally refers to siltstones with high content of ductile components in which climbing ripple lamination is visible.

- (2) Mechanical compaction is the most important destructive diagenesis to reduce the original pore space of Chang 8 sandstone reservoir in shallow-water lacustrine delta, followed by pore-filling calcite in Eodiagenesis and ferrocalcite in Mesodiagenesis, while the deterioration of reservoir quality caused by authigenic kaolinite is limited. Pore-lining chlorite cementation and feldspar dissolution are the major constructive diagenesis. An appropriate amount of pore-lining chlorite conducted to resist the compaction among particles, so as to retain some primary pores. However, excessive chlorite (over 8%) filled the pore or blocked the throats in the form of rosette, leading to the decrease of reservoir petrophysics.
- (3) The diagenetic intensity is related to depositional lithofacies and architectural bounding surface of the reservoir. In the sandstones which are far away from the sandstone-mudstone interface corresponding to lithofacies i, pore-lining chlorite is the most developed cement and significantly enhanced the compression resistance, thus these sandstones experienced widespread feldspar dissolution later. In comparison, sandstones of lithofacies ii with relatively low content of ductile components experienced slightly stronger compaction. However, the sandstones of lithofacies i and lithofacies ii near the sandstone-mudstone interface mostly suffered strong carbonate cementation, and the later dissolution was not well developed. This phenomenon is most common near the bounding surface between channel and mouth bar of the bar finger. Sandstones of lithofacies iii and lithofacies iv with relatively high content of ductile components have experienced strongly continuous compaction after deposited, resulting in almost no reservation of pore space.
- (4) Five different diagenetic evolution patterns of tight sandstones in the digitate shallow-water lacustrine delta were analyzed and summarized, namely pattern I to pattern V, and the relevant reservoir quality successively deteriorates. Compared with the other three diagenetic patterns, the sandstones of pattern I and II tend to form "sweet points" with relatively high permeability under the overall low petrophysics background due to the weakest diagenetic alteration they have experienced, including



**Fig. 23.** Schematic diagram illustrating the distribution and diagenetic evolution patterns in the digitate shallow-water lacustrine delta deposit. (a) The temporal and spatial distribution of various diagenetic alterations among deposits and lithofacies. (b) Characteristics of five conceptual diagenetic evolution patterns at different stages.



moderate compaction, weak carbonate cementation and relatively strong dissolution successively. Pattern I occurs in sandstones of the main part of distributary channels in the upper plain of digitate shallow-water lacustrine delta, which predominates in lithofacies i. Pattern II occurs widely in sandstones of the main part of bar fingers (except for the natural levees and the top of the channel), predominant in lithofacies ii.

### Declaration of competing interest

The authors declare that they have no known competing financial interests or personal relationships that could have appeared to influence the work reported in this paper.

### Data availability

Data will be made available on request.

### Acknowledgements

This study is supported financially by the National Major Science and Technology Projects of China (No. 2017ZX05013-004-002), and the Strategic Cooperation Technology Projects of CNPC and CUPB (No. ZLZX 2020-02). The authors thank PetroChina Changqing Oilfield Company for providing samples and permission to publish the results.

### References

- Aagaard, P., Jahren, J.S., Harstad, A.O., Nilsen, O., Ramm, M., 2000. Formation of grain-coating chlorite in sandstones. Laboratory synthesized vs. natural occurrences. *Clay Miner.* 35 (1), 261–269.
- Wang, G.W., Chang, X.C., Yin, W., Li, Y., Song, T.T., 2017. Impact of diagenesis on reservoir quality and heterogeneity of the Upper Triassic Chang 8 tight oil sandstones in the Zhenjing area, Ordos Basin, China. *Mar. Petrol. Geol.* 83, 84–96.
- Bernard, H.A., 1965. A resume of river delta types: Abstract. *AAPG Bull.* 49.
- Bjørlykke, K., 2014. Relationships between depositional environments, burial history and rock properties. Some principal aspects of diagenetic process in sedimentary basins. *Sediment. Geol.* 301, 1–14.
- Burpee, A.P., Slingerland, R.L., Edmonds, D.A., Parsons, D., Best, J., Cederberg, J., McGuffin, A., Caldwell, R., Nijhuis, A., Royce, J., 2015. Grain-size controls on the morphology and internal geometry of river-dominated deltas. *J. Sediment. Res.* 85, 699–714.
- Chen, L., Lu, Y.C., Wu, J.Y., Xing, F.C., Liu, L., Ma, Y.Q., Rao, D., Peng, L., 2016. Sedimentary facies and depositional model of shallow water delta dominated by fluvial for Chang 8 oil-bearing group of Yanchang Formation in southwestern Ordos Basin, China. *J. Central South Univ.* 22 (12), 4749–4763 (in Chinese with English abstract).
- Chen, H., Zhu, X., Chen, C., Yin, W., Zhang, Q., Shi, R., 2017. Diagenesis and hydrocarbon emplacement in the upper triassic Yanchang Formation tight sandstones in the southern Ordos Basin, China. *Aust. J. Earth Sci.* 64 (7), 957–980.
- Chowdhury, A.H., Noble, P.A., 1996. Origin, distribution and significance of carbonate cements in the albert formation reservoir sandstones, New Brunswick, Canada. *Mar. Petrol. Geol.* 13, 837–846.
- Chu, M.J., Li, S.X., Liu, X.Y., Deng, X.Q., Guo, Z.Q., 2013. Accumulation mechanisms and modes of Yanchang Formation Chang 8 interval hydrocarbons in Ordos Basin. *Acta Sedimentol. Sin.* 31 (4), 683–692.
- Chuhan, F.A., Bjørlykke, K., Lowrey, C., 2000. The role of provenance in illitization of deeply buried reservoir sandstones from Haltenbanken and north Viking Graben, offshore Norway. *Mar. Petrol. Geol.* 17, 673–689.
- Chuhan, F.A., Kjeldstad, A., Bjørlykke, K., Høeg, K., 2003. Experimental compression of loose sands: relevance to porosity reduction during burial in sedimentary basins. *Can. Geotech. J.* 40, 995–1011.
- Deng, X.Q., Lin, F.X., Liu, X.Y., Pang, J.L., Lyu, J.W., Li, S.X., Liu, X., 2008. Discussion on relationship between sedimentary evolution of the triassic Yanchang Formation and the early indosinian movement in Ordos Basin. *J. Palaeogeogr.* 10 (2), 159–166 (in Chinese with English abstract).
- Deng, Q.J., Hu, M.Y., Hu, Z.G., 2019. Depositional characteristics and evolution of the shallow water deltaic channel sand bodies in Fuyu oil layer of central downwarp zone of Songliao Basin, NE China. *Arabian J. Geosci.* 12 (19) <https://doi.org/10.1007/s12517-019-4762-9>.
- Donaldson, C.A., 1969. Ancient deltaic sedimentation (pennsylvanian) and its control on the distribution, thickness, and quality of coals/Some appalachian coals and carbonates: models of ancient shallow-water deposits. *Geol. Soc. Am. Guidebook of Field Trips, Atlantic City, NJ* 93–121.
- Donaldson, C.A., 1974. Pennsylvanian sedimentation of central appalachians. *Spec. Pap. Geol. Soc. Am.* 1148, 47–48.
- Duan, Y., Wang, C.Y., Zheng, C.Y., Wu, B.X., Zheng, G.D., 2008. Geochemical study of crude oils from the Xifeng oilfield of the Ordos Basin, China. *J. Asian Earth Sci.* 31, 341–356.
- Dumars, A.J., 2002. Distributary Mouth Bar Formation and Channel Bifurcation in the Wax Lake Delta, Atchafalaya Bay, Louisiana. Louisiana State Univ., Baton Rouge, p. 88.
- Dutton, S.P., 2008. Calcite cement in Permian deep-water sandstones, Delaware Basin, west Texas: origin, distribution, and effect on reservoir properties. *AAPG Bull.* 92, 765–787.
- Edmonds, D.A., Slingerland, R.L., 2010. Significant effect of sediment cohesion on delta morphology. *Nat. Geosci.* 3, 105–109.
- Edmonds, D.A., Shaw, J.B., Mohrig, D., 2011. Topset-dominated deltas: a new model for river delta stratigraphy. *Geology* 39 (12), 1175–1178.
- Ehrenberg, S., 1989. Assessing the relative importance of compaction processes and cementation to reduction of porosity in sandstones: discussion; compaction and porosity evolution of Pliocene sandstones, Ventura Basin, California: discussion. *AAPG Bull.* 73 (10), 1274–1276.
- Fisher, W.L., Brown, L.F., Scott, A.J., McGowen, J.H., 1969. Delta Systems in the Exploration for Oil and Gas. Bureau of Economic Geology, University of Texas, Austin, TX, p. 78.
- Fisk, H.N., 1954. Sedimentary framework of the modern Mississippi delta. *J. Sediment. Petrol.* 24, 76–99.
- Folk, R.L., 1968. Petrology of Sedimentary Rocks. Hemphill Publishing Co, Austin Texas, pp. 1–170.
- Fu, J.H., Liu, G.D., Yang, W.W., Feng, Y., Zhang, X.F., Cheng, D.X., 2013. A study of the accumulation periods of low permeability reservoir of Yanchang Formation in Longdong Area, Ordos Basin. *Earth Sci. Front.* 20 (2), 125–131.
- Gould, K., Pe-Piper, G., Piper, D.J.W., 2010. Relationship of diagenetic chlorite rims to depositional facies in Lower Cretaceous reservoir sandstones of the Scotian Basin. *Sedimentology* 57 (2), 587–610.
- Grigsby, J.D., 2001. Origin and growth mechanism of authigenic chlorite in sandstones of the lower Vicksburg formation, South Texas. *J. Sediment. Res.* 71, 27–36.
- Henares, S., Caracciolo, L., Viseras, C., Fernandez, J., Yeste, L.M., 2016. Diagenetic constraints on heterogeneous reservoir quality assessment: a Triassic outcrop analog of meandering fluvial reservoirs. *AAPG Bull.* 100, 1377–1398.
- Higgs, K.E., Zwiggmann, H., Reyes, A.G., Funnell, R.H., 2007. Diagenesis, porosity evolution, and petroleum emplacement in tight gas reservoirs, Taranaki Basin, New Zealand. *J. Sediment. Res.* 77 (12), 1003–1025.
- Hillier, S., 1994. Pore-lining chlorites in siliciclastic reservoir sandstones – electron-microprobe, SEM and XRD data, and implications for their origin. *Clay Miner.* 29 (4), 665–679.
- Hu, C.H., Qu, H.J., Miao, J.Y., Wang, W.L., Ma, Q., 2008. A study on sedimentary microfacies and oil-bearing possibility in Chang 6 oil-bearing formation in the area of Nannivan. *J. Northwest For. Univ.* 38 (6), 994–1000 (in Chinese with English abstract).
- Hu, Y., Huang, K., Xu, Z.H., Zhao, J.S., Wu, J.C., 2019. Distribution character of remaining oil with finger bar of bird-foot shoal water delta reservoir in BZ oilfield, Bohai Bay Basin. *Geol. Sci. Technol. Inf.* 38 (2), 189–198 (in Chinese with English abstract).
- Qiao, J.C., Zeng, J.H., Jiang, S., Wang, Y.N., 2020. Impacts of sedimentology and diagenesis on pore structure and reservoir quality in tight oil sandstone reservoirs: implications for macroscopic and microscopic heterogeneities. *Mar. Petrol. Geol.* 111, 279–300.
- Jahren, J.S., 1991. Evidence of Ostwald Ripening related recrystallization of diagenetic chlorites from reservoir rocks offshore Norway. *Clay Miner.* 26, 169–178.
- Jopling, A.V., 1966. Some applications of theory and experiment to the study of bedding genesis. *Sedimentology* 7, 71–102.
- Lai, J., Wang, G.W., Ran, Y., Zhou, Z.L., Cui, Y.F., 2016. Impact of diagenesis on the reservoir quality of tight oil sandstones: the case of Upper Triassic Yanchang Formation Chang 7 oil layers in Ordos Basin, China. *J. Petrol. Sci. Eng.* 145, 54–65.
- Li, Z., Wu, S.H., Xia, D.H., Zhang, X.F., Huang, M., 2017. Diagenetic alterations and reservoir heterogeneity within the depositional facies: a case study from distributary-channel belt sandstone of Upper Triassic Yanchang Formation reservoirs (Ordos Basin, China). *Mar. Petrol. Geol.* 86, 950–971.
- Liu, Z., Zhu, X., Liao, J., 2013. Sequence stratigraphy and genesis of sand bodies of the upper Triassic Yanchang formation in the southwestern margin of Ordos Basin. *Earth Sci. Front.* 20 (2), 1–9.
- Liu, H.P., Zhao, Y.C., Luo, Y., Xiao, G.J., Meng, Y.J., Zhou, S.B., Shao, L.K., 2020. Origin of the reservoir quality difference between Chang 8 and Chang 9 member sandstones in the honghe oil field of the southern Ordos Basin, China. *J. Petrol. Sci. Eng.* 185 <https://doi.org/10.1016/j.petrol.2019.106668>.
- Loucks, R.G., Dodge, M.M., Galloway, W.E., 1984. Regional Controls on Diagenesis and Reservoir Quality in Lower Tertiary Sandstones along the Texas Gulf Coast: Part 1. Concepts Print, pp. 14–45.
- Ma, C.L., Wang, R.J., Luo, B.L., Duan, W.B., Feng, C.Y., Wang, S.P., Suo, Y.X., Qiang, Z.Z., 2012. Characteristics of chang-8 oil reservoir and distribution of oil reservoirs in maling oilfield, Ordos Basin. *Nat. Gas Geosci.* 23 (3), 514–519 (in Chinese with English abstract).
- McHargue, T.R., Price, R.C., 1982. Dolomite from clay in argillaceous limestones or shale associated marine carbonates. *J. Sediment. Res.* 52, 873–886.
- Melezhik, V.A., Fallick, A.E., Smirnov, Y.P., Yakovlev, Y.N., 2003. Fractionation of carbon and oxygen isotopes in C-13-rich Palaeoproterozoic dolostones in the transition from medium-grade to high-grade greenschist facies: a case study from the kola superdeep drillhole. *J. Geol. Soc.* 160, 71–82.

- Nedkvitne, T., Karlsen, D.A., Bjørlykke, K., Larter, S.R., 1993. Relationship between reservoir diagenetic evolution and petroleum emplacement in the Ula Field, North Sea. *Mar. Petrol. Geol.* 10, 255–270.
- Neveux, L., Grgic, D., Carpentier, C., Pironon, J., Girard, J.P., 2014. Influence of hydrocarbon injection on the compaction by pressure solution of a carbonate rock: an experimental study under triaxial stresses. *Mar. Petrol. Geol.* 55, 282–294.
- Olariu, C., Bhattacharya, J.P., 2006. Terminal distributary channels and delta front architecture of river-dominated delta systems. *J. Sediment. Res.* 76, 212–233.
- Postma, G., 1990. An analysis of the variation in delta architecture. *Terra. Nova* 2, 124–130.
- Rossi, C., Alaminos, A., 2014. Evaluating the mechanical compaction of quartzarenites: the importance of sorting (Llanos foreland basin, Colombia). *Mar. Petrol. Geol.* 56, 222–238.
- Trendell, A.M., Atchley, S.C., Nordt, L.C., 2012. Depositional and diagenetic controls on reservoir attributes within a fluvial outcrop analog: upper Triassic Sonsela member of the Chinle formation, petrified forest national park, Arizona. *AAPG Bull.* 96 (4), 679–707.
- Wang, W., Jiang, Y., Swennen, R., Yuan, J., Liu, J., Zhang, S., 2018. Pore-throat characteristics of tight sandstone reservoirs composed of gravity flow sediments: yingcheng Formation, Longfengshan sag, China. *J. Petrol. Sci. Eng.* 171, 646–661.
- Wang, J.J., Wu, S.H., Li, Q., Xiao, S.M., 2020. Controls of diagenetic alteration on the reservoir quality of tight sandstone reservoirs in the Triassic Yanchang formation of the Ordos Basin, China. *J. Asian Earth Sci.* 200, 104472.
- Woo, K.S., Kim, B.K., 2006. Stable oxygen and carbon isotopes of carbonate concretions of the Miocene Yeonil Group in the Pohang Basin, Korea: types of concretions and formation condition. *Sediment. Geol.* 183, 15e30.
- Xu, Z.H., Wu, S.H., Liu, Z., Zhao, J.S., Wu, J.C., Geng, L.H., Zhang, T.Y., Liu, Z.W., 2019. Reservoir architecture of the finger bar within shoal water delta front: insights from the lower member of minghuazhen formation, neogene, Bohai BZ25 oilfield, Bohai Bay Basin, east China. *Petrol. Explor. Dev.* 46, 1–12.
- Wu, S.H., Xu, Z.H., Liu, Z., 2019. Depositional architecture of fluvial-dominated shoal water delta. *J. Palaeo. (Chinese Edition)* 21 (2), 202–215. <https://doi.org/10.7605/gdxb.2019.02.012>.
- Xu, Z.H., Plink-Bjorklund, P., Wu, S.H., Liu, Z., Feng, W.J., Zhang, K., Yang, Z., Zhong, Y. C., 2022. Sinuous bar fingers of digitate shallow-water deltas: insights into their formative processes and deposits from integrating morphological and sedimentological studies with mathematical modelling. *Sedimentology* 69 (2), 724–749.
- Yang, Y.X., Huang, Q., Liu, W.T., Liu, Q., Wang, B., Wang, Y., 2015. Research of reservoir heterogeneity of shallow-water delta system, Ordos Basin: taking Chang 8 reservoir in Maling Oilfield as an example. *Complex Hydrocarbon Reservoirs* 8 (3), 39–43 (in Chinese with English abstract).
- Yao, S.P., Zhang, K., Hu, W.X., Fang, H.F., Jiao, K., 2009. Sedimentary organic facies of the triassic Yanchang Formation in the Ordos Basin. *Oil Gas Geol.* 30, 74–84 (in Chinese with English abstract).
- Yao, J.L., Deng, X.Q., Zhao, Y.D., Han, T.Y., Chu, M.J., Pang, J.L., 2013. Characteristics of tight oil in triassic Yanchang Formation, Ordos Basin. *Petrol. Explor. Dev.* 40 (2), 161–169.
- Yin, T., Li, X., Zhang, C., Zhu, Y., Gong, F., 2012. Sandbody shape of modern shallow lake basin delta sediments: by taking Dongting Lake and Poyang Lake for example. *J. Oil Gas Technol. (J. Jiangnan Petroleum Inst.)* 34 (10), 1–7.
- Yue, D., Wu, S., Xu, Z., Xiong, L., Chen, D., Ji, Y., Zhou, Y., 2018. Reservoir quality, natural fractures, and gas productivity of upper Triassic Xujiache tight gas sandstones in western Sichuan Basin, China. *Mar. Petrol. Geol.* 89, 370–386.
- Zhang, J.L., Si, X.Q., Liang, J., Lin, H., 2004. Diagenesis of lacustrine deltaic sandstone and its impact on reservoir quality. *Acta Sedimentol. Sin.* 22 (2), 225–233.
- Zhang, J., Wang, M., Wang, Y., Jiang, Y., Lei, Y., Zhang, L., Wang, J., 2017. Identification and sedimentary evolution of the shallow water delta of bird-foot in bozhong 28–2S oilfield group of Bohai Bay Basin. *Period. Ocean Univ. China* 47 (9), 77–85 (in Chinese with English abstract).
- Zhang, L., Bao, Z.D., Dou, L.X., Xu, Q.H., 2021. Diagenetic alterations related to sedimentary architecture of deltaic distributary channels in red beds of the Cretaceous Yaojia Formation, Songliao Basin. *J. Petrol. Sci. Eng.* 203, 108564.
- Zhou, Y., Ji, Y.L., Xu, L.M., Che, S.Q., Niu, X.B., Wan, L., Zhou, Y.Q., Li, Z.C., You, Y., 2016. Controls on reservoir heterogeneity of tight sand oil reservoirs in Upper Triassic Yanchang Formation in Longdong Area, southwest Ordos Basin, China: implications for reservoir quality prediction and oil accumulation. *Mar. Petrol. Geol.* 78, 110–135.
- Zhu, X.M., Deng, X.Q., Liu, Z.L., Sun, B., Liao, J.J., Hui, X., 2013. Sedimentary characteristics and model of shallow braided delta in large-scale lacustrine: an example from Triassic Yanchang Formation in Ordos Basin. *Earth Sci. Front.* 20 (2), 19–28.
- Zhu, X.M., Zeng, H.L., Li, S.L., Dong, Y.L., Zhu, S.F., Zhao, D.N., Huang, W., 2017. Sedimentary characteristics and seismic geomorphologic responses of a shallow-water delta in the Qingshankou Formation from the Songliao Basin, China. *Mar. Petrol. Geol.* 79, 131–148.
- Zou, C.N., Zhang, X.Y., Luo, P., Wang, L., Luo, A., Liu, L.H., 2010. Shallow-lacustrine sand-rich deltaic depositional cycles and sequence stratigraphy of the upper triassic Yanchang Formation, Ordos Basin, China. *Basin Res.* 22 (1), 108–125.